AUS Repository

3D Printing Technology Utilizing Available Construction Materials in the UAE

Item Type	Thesis
Authors	Ahmed, Sara Khaled
Download date	2026-02-10 05:30:52
Link to Item	http://hdl.handle.net/11073/16574

3D PRINTING TECHNOLOGY UTILIZING AVAILABLE CONSTRUCTION MATERIALS IN THE UAE

by

Sara Khaled Ahmed

A Thesis presented to the Faculty of the
American University of Sharjah
College of Engineering
In Partial Fulfillment
of the Requirements
for the Degree of

Masters of Science in
Civil Engineering

Sharjah, United Arab Emirates

November 2019

© 2019 Sara Khaled Ahmed. All rights reserved.

Approval Signatures

We, the undersigned, approve the Master's Thesis of Sara Khaled Ahmed

Thesis Title: 3D Printing Technology Utilizing Available Construction Materials in the UAE

Signature	**Date of Signature** (dd/mm/yyyy)
___________________________ Dr. Sherif Yehia Professor, Department of Civil Engineering Thesis Advisor	_______________
___________________________ Dr. Farid Abed Professor, Department of Civil Engineering Thesis Committee Member	_______________
___________________________ Dr. Lotfi Romdhane Professor, Department of Mechanical Engineering Thesis Committee Member	_______________
___________________________ Dr. Irtishad Ahmad Head, Department of Civil Engineering	_______________
___________________________ Dr. Lotfi Romdhane Associate Dean for Graduate Affairs and Research College of Engineering	_______________
___________________________ Dr. Naif Darwish Acting Dean, College of Engineering	_______________
___________________________ Dr. Mohamed El-Tarhuni Vice Provost for Graduate Studies	_______________

Acknowledgement

I would like to express my sincere gratitude to my advisor Dr. Sherif Yehia for his guidance, motivation, and immense knowledge throughout my research stages. His passion and enthusiasm have always inspired me to do more.

I take this opportunity to express gratitude to all the professors of the Civil engineering program who taught me the undergraduate and graduate level courses with mighty teaching methods and skills. I would also like to thank my committee members, Dr. Farid Abed, and Dr. Lotfi Romdhane for their beneficial feedback and valuable comments.

I extend thanks to the American University of Sharjah for awarding me the Graduate Teaching/Research Assistantship which helped me pursue my Master's degree. I would like to thank our lab instructor Mr. Arshi Faridi for his great assistance in the lab. I would also like to thank Dr. Aqeel Ahmed and Mr. Riyadh for clarifying some of my doubts while working on this thesis. I am very appreciative to all those who have helped me in the lab work, particularly, Eng. Yazan, and Eng. Mohammed Ansari.

Last but not least, I would like to express my deepest appreciation for all those who have helped me throughout this process. If it were not for my close ones, family and friends, after Allah's blessings, this work would not have been possible.

Abstract

Over the past decade, rapid developments in 3D printing technology was observed within the construction industry. 3D printing is an innovative construction technique which may be referred to as automated construction, digital or additive manufacturing. This technology has the ability to build complex structures with no formworks, reduces construction costs and material usage, which will allow for the adoption of a sustainable built environment. However, there are still many challenges that limit the capabilities of 3D printing. To develop concrete which is pumpable, extrudable, and buildable, the workability of the fresh printing concrete is the key factor that has to be evaluated and monitored over time. This study aims to develop a 3D printing concrete using locally available materials and to asses it in terms of its fresh properties. The experimental program involved two phases. In phase 1 evaluation two groups of mixes were developed mainly to examine the effect of supplementary cementitious materials (Ground-granulated blast-furnace slag and Silica fume) on the extrudability and compressive strength. The optimal mix of phase one was found to be the mix containing both crushed and dune sand, and GGBS and SF combined. In phase 2 evaluation, the optimal mix was selected from phase 1, and was developed with three different aggregate to binder (*a/b*) ratios of 1.2, 1.5, and 1.8. The evaluation criteria included the extrudability, setting-time, open-time, workability, and buildability of the mixes. The workability was assessed in terms of the penetration, slump, and flow. The results of phase two suggest that the extrudability was best monitored with the flow test as compared to the slump and penetration tests. The optimal slump and flow percentage ranges that maintain acceptable extrudability were 85-0 mm and 90-45%, whereas, the buildability was performed at a slump and flow of 45-50 mm and 66%. The increase in a/b ratio led to mixes with higher buildability. Finally, the compressive strength of printed specimens of phase 2 mixes was also evaluated and the results demonstrated that the strength of the specimens decreased with the increase in a/b ratio.

Keywords: ***Additive Manufacturing; Contour Crafting; D-Shape; Concrete Printing; Cementitious Materials; Thixotropy, Extrudability; Flowability; Open-time; Buildability; Anisotropy*.**

Table of Contents

List of Figures

List of Tables

List of Abbreviation

AM	Additive Manufacturing
ASTM	American Society for Testing and Materials
BLS	Bureau of Labor Statistics
CAD	Computer Aided Design
CC	Contour Crafting
CFOI	Census of Fatal Occupational Injuries
CLFDM	Curved layered Fused Deposition Modeling
ESA	European Space Agency
FDM	Fused Deposition Modeling
NASA	National Aeronautics and Space Administration
SLA	Stereolithography
SRA	Shrinkage Reducing Agent
TU/e	Eindhoven University of Technology
VMA	Viscosity Modifying Agent
WASP	World’s Advanced Saving Project

Chapter 1. Introduction

The 3D printing technology has the potential to provide solution for many of the problems the construction industry is facing. In this chapter, a brief overview of the use of concrete in the building industry and the problems encountered during construction are presented. The thesis objectives and research contribution are then outlined followed by the general organization of the thesis.

1.1 Overview

With the ongoing developments the world is facing, concrete remains the most widely used building material up to date ever since ancient Egypt. It compromises about 60% of the built environment in many of the developed countries [1]. This is mainly because of the versatility, durability, and economy of concrete when compared to other building materials. Durability is the ability of concrete to resist chemical attack, abrasion, weathering action and other forms of deterioration [1]. Concrete is also fire resistant, non-combustible, and does not fuel like fire. It is used in a variety of different applications in the construction industry such as in, buildings, dams, bridges, roads, electric poles, reservoirs, canals, retaining walls etc. Concrete compromises mainly of aggregates, cement, and water. In addition to these three main components, a variety of other materials such as, additives, superplasticizers, aggregates, or cementitious materials could be added to enhance the concrete's properties and to make it a more durable and sustainable concrete. Many of these compositions are already used in practice with many more still being investigated outside practice.

Despite these advantages there are several drawbacks related to the construction industry that have always been the focus of other researches. First, the construction industry is a high-risk industry, which employs a large number of workers that are involved in wide range activities that often become victims of serious diseases and injuries. The Census of Fatal Occupational Injuries (CFOI) released by the Bureau of Labor Statistics (BLS) showed that the construction industry was responsible for the death of 937 workers in 2015. The main causes of fatalities are due to accidental falls/slips/trips, contact with objects/equipment, and exposure to harsh substances or environments [2]. The percentages of construction worker fatalities by event or exposure is demonstrated in Figure 1.1. Second, the cement, which is a main ingredient in concrete, is considered the third-largest source of anthropogenic carbon dioxide (CO_2) emissions after fossil fuel and land-use change. The production of cement emits CO_2 both directly and indirectly. Directly by the heating of limestone, which occurs through a chemical reaction known as calcination, and indirectly by the burning of fossil fuels to heat the kiln, which is heated, by coal, natural gas, or oil. Cement contributes to about 5% of the global anthropogenic CO_2 emissions [3]. Third, the production and use of formworks for concrete is one of the major obstacles faced by the construction environment. Usually, most projects are required by the clients to reduce construction costs. This is usually achieved by the selection of a system of well-designed and efficient formwork. Formwork limit both diversification and the production of very complicated structural components. There are different types of formwork used that are made up of timber, aluminum, steel, and plastic. The objectives that should be satisfied by the formworks are the safety, quality, speed, and economy. Whichever formworks are used there are always limitations regarding the time needed for the setup of the formwork on site, the number of times the formwork material can be reused, limitations in sizes and shapes, etc. Rapid development in technologies have led to the emergence of three-dimensional (3D) printers, which today have the ability to print concrete structures. This technology has the potential to address many of the problems the construction industry is facing, such as the problems discussed above.

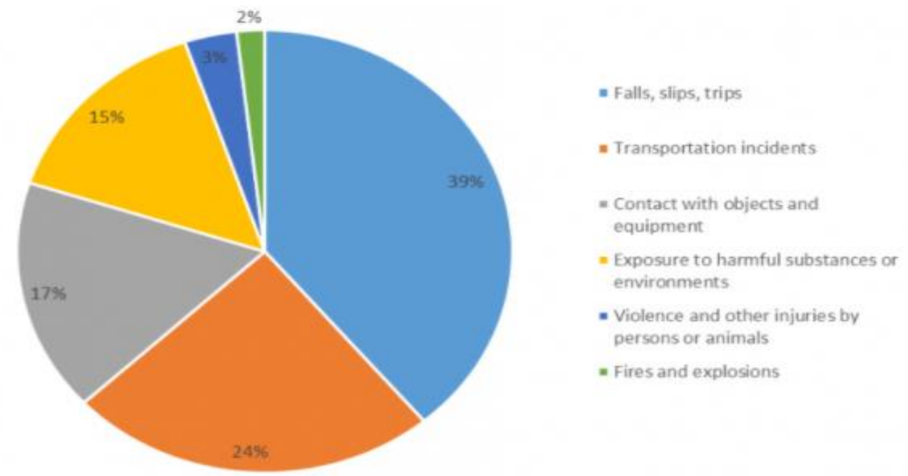

Figure 1.1: Construction worker fatalities by event or exposure [2]

1.2. Thesis Objectives

The 3D printing technology is gaining ground in the building industry. This have led to the urge of studying the printing concrete properties and to investigate guidelines and acceptance criteria to accept the printing concrete. Some research efforts provided information on some of the significant characteristics of the printing concrete. To achieve universal acceptance criteria, still numerous amounts of research is still required in this area. The main goal of this study is to prepare mixes for 3D printing utilizing local construction materials available in UAE. In addition, evaluate the fresh printing concrete properties which are the extrudability, setting-time, open-time, buildability, and compressive strength using devices commonly used in the construction industry. The objectives to satisfy this goal are as follows:

- Develop different 3D printing concrete mixes using the locally available materials in the UAE to evaluate their effect on the fresh properties of the printing concrete.
- Evaluate the change of workability with time using the Vicat needle penetration, slump, and mortar flow test.
- Monitor the extrudability with time along with the penetration, slump, and flow, to determine the ranges that maintain acceptable printing quality.
- Determine the optimal range of slump and percentage flow that satisfy the buildability.
- Perform correlation analysis to determine the strength of the relationship between each of the penetration, slump, and flow with time, since the extrudability is time dependent.
- Develop a prediction model based on the best workability indicator to determine the range at which extrudability will not be satisfied for the mixes investigated in this research and validate the model.
- Determine the effect of the layering process on the compressive strength of the concrete by comparing printed specimens with cast specimens of different concrete mixes.

1.3. Research Contribution

Even though the amount of research conducted for 3D printing in construction is exponentially increasing, the research in this area is still considered very limited.

Continuous research is needed at a variety of levels to address many of the challenges that limit the capabilities of this innovative technology. Different test methods to express the workability/flowability of printing concrete still need to be investigated. The contribution of this research can be summarized as follows:

- The effect of different aggregate to binder ratios on the extrudability, setting-time, open time, workability, buildability and compressive strength will be investigated.
- The workability of the printing concrete will be assessed in terms of penetration, slump and flow, and will be monitored over time along with the extrudability to determine the ranges at which extrudability is satisfied.
- Correlation analysis will be conducted to find the correlation between each of the workability indicators (penetration, slump, and flow) with time, as well as to find their mutual relationship strengths to validate the experimental results.
- The best workability indicator will be selected and based on it, a prediction model will be developed to check the workability at which different mixes with different aggregate to binder ratios do not satisfy the extrudability criteria.
- The effect of the layering process on the concrete strength will be determined.

1.4. Thesis Organization

The remaining parts of the thesis are organized as follows. Chapter 2 presents the background and literature review of 3D printing. In this chapter, the history of 3D printing in construction is outlined. The most commonly used techniques of 3D printing are illustrated along with some noteworthy examples. The fresh and hardened properties that are required to be achieved by the printing concrete are also discussed. The experimental procedures followed by the research project to achieve the objectives are then proposed in Chapter 3. Chapter 4 presents and discusses the experimental results. Finally, Chapter 5 summarizes and concludes the findings of this research and proposes future works.

Chapter 2. Background and Literature Review

The 3D printing technology was introduced when Charles Hull invented the first 3D printing technology, Stereolithography (SLA) in 1986. The technology has been used in a variety of domains such as in medicine, manufacturing, and food industries; however, its use was only limited to small scale applications. In fact, it was not until the mid-1990s, that the building industry adopted this technique and aimed to apply it to large-scale applications. The 3D printing technology has the potential to reduce the construction time and material usage, provide a larger variety of customized homes and building, eliminate the usage of formwork, minimize the chances of error due precise material deposition, and increase the levels of safety in construction. It can allow for reduced construction costs, as the structural elements in buildings are no longer required to be identical to save time or money. In addition, the ability of this technology to print different components in an efficient way will also allow for the adoption of a sustainable built environment.

The 3D printing technology works in such a way that it adds layer upon layer, which is why it is also known as Additive Manufacturing (AM) technology. It is defined by American Society for Testing and Materials (ASTM) as 'the process of joining materials to make objects from 3D model data, usually layer upon layer' [4]. At first, a 3D model has to be developed using any 3D modeling software such as Computer Aided Design (CAD). This model then has to be sliced using a slicing software, which slices the 3D model into hundreds or thousands of horizontal layers. Once the 3D model is sliced, it can then be sent to the printer via Bluetooth, Wi-Fi, etc., and printed layer upon layer. In general, 3D printers differ from one another by the printing procedure, and the materials that can be fed into the printer to construct the desired 3D model.

2.1. Outline of the 3D Printing History in Construction.

The first cement-based additive manufacturing was initiated by Joseph Pegna in 1997. Complex samples of masonry structures that could not be cast were manufactured through an incremental deposition of sand and Portland cement. First, a thin layer of sand is deposited, followed by the deposition of patterned layer of cement. Steam is then applied to the layer to achieve rapid curing. The main concept demonstrated by Pegna was that the fabrication of complicated shapes could be achieved through many simple operations to get the desired 3D shape [5]. This work however was not continued, and another cementitious material AM process known as Contour Crafting was developed by Berokh Khoshnevis in 1998. Contour Crafting (CC) is an automation process, which uses layered fabrication. It is one of the best techniques available to date which can print large structures such as houses. This technique prints structures through the deposition of cementitious concrete layer by layer by a gantry-driven nozzle which requires no formwork to be used [6, 7]. Another 3D printer known as D-Shape was invented in 2007 by an Italian civil engineer known as Enrico Dini. This is a powdered-based printer which prints layer by layer using sand and inorganic powder to produce construction elements used in architectural masonry, landscaping elements, and maritime projects [8]. More details about the Contour Crafting and D-Shape will be discussed in the following section. A different approach was developed by Platt in 2013, which uses cellular fabrication (C-Fab) technology. This technology does not print whole structures and limits itself only to printing specific structural components such as walls. Currently, it can only be used for building supports structures for building components. Platt informed that his firm is seeking to minimize the 3D printing aspect of his technology, and only use additive manufacturing where necessary. Due to this, C-Fab may have the potential to be adopted in the modern construction industry more quickly and affordably than other 3D printing technologies [9]. The Fused Deposition Modeling (FDM) is a famous technique in the additive manufacturing world. FDM was developed by Stratasys in Eden Prairie in 1992 and uses plastic or wax material as the building material. The plastic is melted to a temperature that is right above its melting point to facilitate its flow through the nozzle to form layers. Other materials include, polyamide, polycarbonate, polyethylene, polypropylene, and investment casting wax [10]. In 2014, a Chinese Company, Qingdao Unique Technology, adopted a large 3D printer of size 12mx12mx12m which uses a similar technology to the FDM. The process prints through extruding layers of half-melt glass reinforced plastic material to create the prototypes. It aims to print the 'Temple of Heaven', which is the largest extant sacrificial temple in China [11-13]. In 2015, a huge 3D printer known as Big Delta was developed by the World's Advanced Saving Project (WASP). The main aim of this company is to print structures using eco-friendly materials. It printed an adobe structure using clay, dirt, straw and water [14].

2.2. Printing Procedures Available in Construction.

As discussed, when automation first appeared, it prevailed in almost all domains except for the construction industry. Previously, the adoption of this technique in construction was slow because at that time the automated fabrication technologies were not suitable for large scale applications, materials used in automation systems were limited, and the automated equipment were economically unattractive [7]. A new approach known as rapid prototyping (RP) appeared in the late 1980s, which used layered fabrication. This approach paved the way for the application of 3D printing in construction, and since then new techniques, which use layered fabrication have been constantly developed. Three techniques that have the potential to be applied in real life construction are the Contour Crafting, D-shape, and Concrete printing. Each of these techniques will be discussed briefly in this section.

2.2.1. Contour crafting. The Contour Crafting (CC) is the first rapid prototype additive fabrication technology that allowed for the construction of large-scale structures. It uses computer control to exploit the superior surface forming capability of troweling to create smooth and accurate planar and free form surfaces. Some of its benefits include better surface quality, higher fabrication speed, and a wider selection of materials. The printing nozzle moves along the X and Z direction by a gantry system. Two parallel sliding structures carry and move the nozzle along the Y direction. A schematic plot shown in Figure 2.1 depicts the contour crafting in construction. Figure 2.2 demonstrates the extrusion nozzles. Two trowels are usually used for the creation of smooth and accurate surfaces for the object being created. If needed, the side trowel can dynamically be deflected to create non-orthogonal surfaces. This method involves an extrusion and filling process, which is illustrated in Figure 2.3. The extrusion process builds only the outer edges of the object surface, and the filling process builds the object core using any filler material such as concrete. This process also includes automated reinforcement, automated plumbing, automated electrical network installation, etc., which is done by the integration of robotic modules. Projections estimated that the costs will be around one fifth of conventional construction [6, 7, 15].

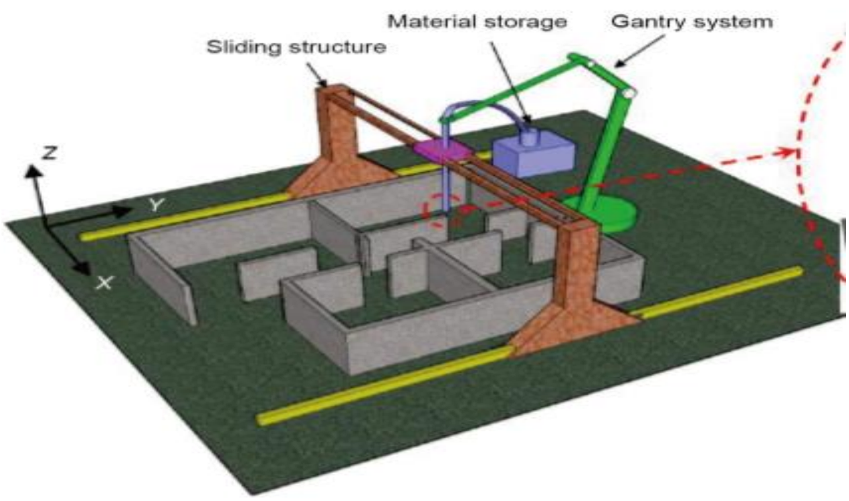

Figure 2.1: Schematic plot for contour crafting [16]

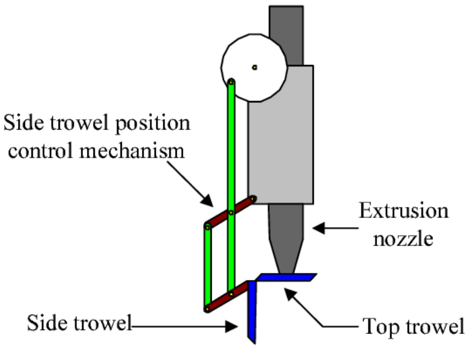

Figure 2.2: Extrusion nozzle [6]

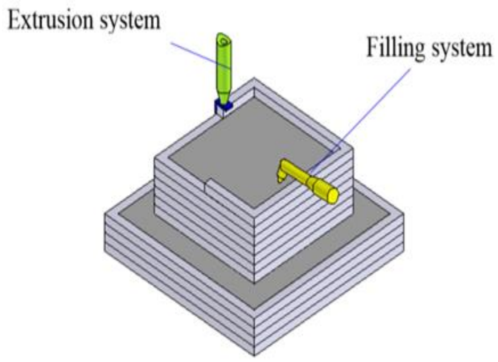

Figure 2.3 Extrusion and filling processes [6]

Rapid advances on enhancing the CC's superior surface forming capability, speed, part size, and nozzle dimensions are still ongoing. This technology has already been used on site. Some of the noteworthy examples are depicted in Figure 2.4. The castle was built from sand and cement in Minnesota, USA, by Total Kustom in 2014 [17]. The five-story apartment building was built in Suzhou, China, by the WinSun company, in 2015 [18]. The office of the future, the world's first office, in Dubai, UAE, was also built by the WinSun company [19]. The National Aeronautics and Space Administration (NASA) have gained interest in this technology, and currently aim to apply it on Mars and the Moon, using concrete Sulphur and moon soil (regolith) to build habitats.

a) Castle [16] b) Five-storey building [18] c) office [20]

Figure 2.4: Examples of contour crafting.

2.2.2. D-Shape. The D-Shape process is a dry process, which selectively binds sand with inorganic powder to produce stone like structures. It is claimed that the D-Shape can generate objects that are indistinguishable from marble. A schematic plot of the D-Shape printer is shown in Figure 2.5. The machine consists of a square frame, a large flat bed, and a horizontal beam, which has the printer head installed in it with up to 300 nozzles. The horizontal beam with the nozzles moves along the X direction, and the square base moves by a four-stepper motor along the Z direction. In the printing process, a layer of build material such as sand is spread out to the desired thickness, and then inorganic binder is deposited through the nozzles on the predefined area on the sand layer. Once a layer is formed, the remaining sand, which was not bind, is left for the formation of the subsequent layer. The D-shape is used for printing houses or building blocks [8, 21].

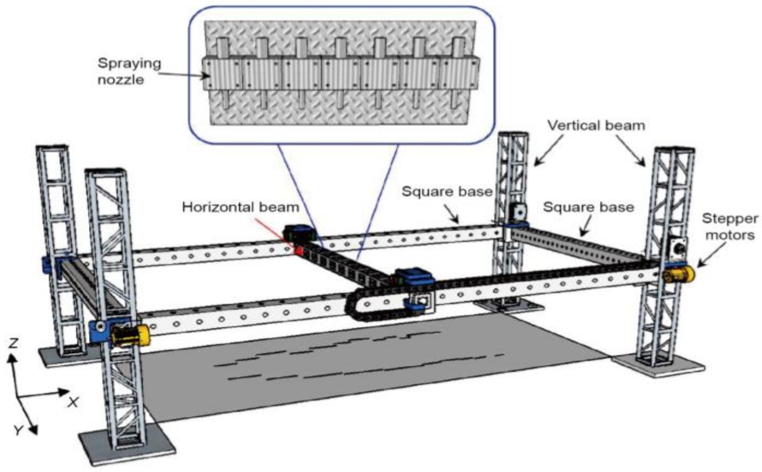

Figure 2.5: Schematic plot for D-shape printing [16]

Some of the structures that were printed using the D-Shape are illustrated in Figure 2.6. The landscape house was developed by the Universe Architecture and contractor BAM in Amsterdam, the Netherlands [22]. Research funded by the European Space Agency (ESA) aim to explore the possibility of using the 3D printing technology (D-Shape) for building habitats on the Moon using regolith [23].

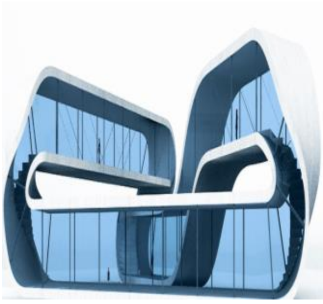

a) Landscape house [16]

b) sculpture [16]

c) House built in a single process [23]

Figure 2.6: Examples of D-Shape.

2.2.3. Concrete printing. Similar to the contour crafting, the concrete printing is based on the extrusion of cement mortar. It has a smaller resolution of deposition which gives it better control of internal and external geometries as compared to the CC [24]. A schematic plot of the concrete printing is shown in Figure 2.7. The machine is quite similar to the CC machine; however, here the nozzles are designed to move in the X, Y and Z directions via steel beams. A material container stores the concrete is mounted on top of the print head. Concrete is then delivered through the delivery pipe to the nozzle by a pump. Continuous filaments are then extruded from the nozzle to form the 3D component.

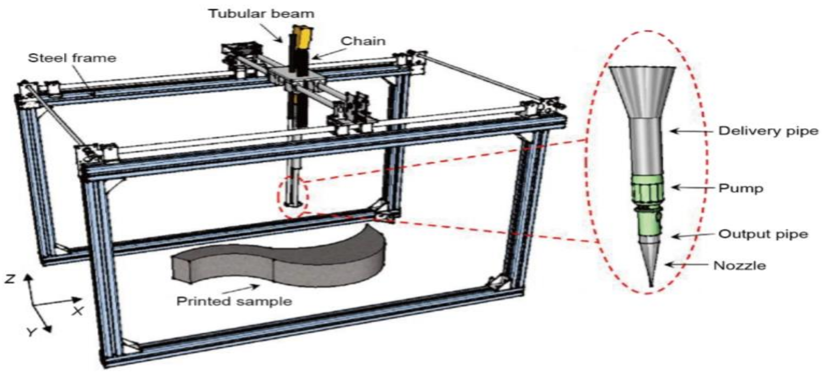

Figure 2.7: Schematic plot for concrete printing [16]

A concrete printing machine was developed at the Loughborough University which operates within a 5.4mx4.4mx5.2m steel frame [25]. A high-performance concrete was developed for this technique. A research team at the Eindhoven University of Technology (TU/e) have revealed the details of their massive printer in 2017 which has a print area of 9mx4.5mx3m [22]. Examples of the concrete printing technique are depicted in Figure 2.8. The printed bench was printed by the Le et al [25]. The printed doubly curved 4-part sandwich was developed by Lim et. al [26]. The model was printed by a non-conventional method of 3D printing and Curved Layered Fused Deposition Modeling (CLFDM) was used.

a) Printed bench [25]

b) Printed doubly curved 4-part sandwich panel [26]

Figure 2.8: Examples of concrete printing.

2.3. Current Status of 3D Printing Construction in UAE.

Considerable efforts has been observed from contracting companies in UAE ever since Sheikh Mohammad Bin Rashid announced Dubai's 3D Printing Strategy in 2016. The strategy is to make Dubai the world's 3D printing hub by year 2030. The strategy's aim is to help reduce costs particularly in medical and construction sectors by adopting this emerging technology. It is expected by Dubai Municipality's regulation that all new buildings will be around 25% 3D printed by 2025. This move is expected to start from 2019 with 2% gradual increase until the goal is achieved [27]. Two companies which are expected to contribute towards Dubai's 3D Printing Strategy are Concreative and Acciona [28]. Concreative is the first large-scale 3D pinting company in UAE. The aim of this company is to structural and architectural components which cannot be constructed using conventional methods. The company uses a large-scale concrete 3D printer which was developed by their partner XtreeE in France. The 6-axis arm 3D printer can print components with up to 3m height and 5m length in one shot [29]. Acciona is a Spanish conglomerate group which is dedicated to infrastructural management. The company adopted a large scale concrete 3D printer, 6X3X2 m in size, which is suitable for architectural, urban and building applications [30].

Projects implemented in Dubai include the 3D printed office (see Figure 2.4c), 3D printed lab, and 3D printed two-storey building. The 3D printed office is the most advanced 3D printed building in the world. The duration of the project was, 17 days for printing, 3 days for installation, and approximately 3 months for building services, interiors, and landscape. The labour cost was cut by almost 50% compared to conventional building methods for building the same house. More details are available on [20]. The DEWA lab is the first lab to be 3D printed in the world, and first building in Dubai to be built completely on-site. The lab has a capacity of 132 m^2 and consists of 4 sub laboratories which include an electronic lab, a software lab, a mechanical lab, and a prototype lab. The science of unmanned aerial vehicles and 3D printing will be studied in the lab [31]. Dubai has also revealed the world's largest 3D printed two-storey building in 2019. This project is considered a turning point in the construction sector. The building has a total area of 640 m^2 and is 9.5m high and was built using an on-site 3D printing equipment with local components. It has been reported that the construction costs were cut from DHS2.5 million to DHS1 million. The workers involved were 50% less than the usual, and about 60% less waste was generated [32]. The two-storey building is shown in Figure 2.9 The Cybe Construction is another company which is a Dutch specialist in 3D printing which is currently working on 3D printing houses in Sharjah. The first house to be printed will be used as part of Sharjah Research, Technology and Innovation Park (SRTI Park). The goal is to build different types of buildings to make Sharjah an architectural hub [33].

Figure 2.9: Dubai's two-storey building [32].

2.4. Cementitious Materials for 3D Printing.

2.4.1 Fresh printing concrete properties. The material selected for 3D printing plays a very crucial role for the development of high quality and high-performance printed structures. In general, the concrete used for printing has to have an acceptable extrudability to be deposited out of the nozzles in the printer head. The filaments deposited out of the nozzles has to be extruded in a continuous manner without blockage. The filaments extruded have to maintain their shape once extruded from the nozzle, should remain active and stay viscous to ensure sufficient bonding between the filaments to form layers, and should have enough stiffness to retain its extruded shape under its self-weight and upper layers.

In this subsection, first literature on some of the earlier studies which provided an initial understanding of the printing concrete will be presented followed by a discussion on the rheology of fresh concrete, interlayer strength, and mechanical properties. A summary on the fresh printing concrete evaluation from the literature is presented in Table 1.1.

2.4.1.1. Examination of fresh properties by earlier studies. The 3D printing technology is still in its initial stages and thus it is essential to investigate the use of different materials on these specific characteristics, and to investigate guidelines for evaluating the proposed mixtures or materials. Le et al. [25] proposed a way for developing printing concrete and developed a high-performance printing concrete with a compressive strength of 110 MPa using their laboratory concrete printing machine, which operates within a 5.4m x 4.4m x 5.4m steel frame. The extrudability and buildability were found to be the most crucial fresh concrete printing properties, which have a mutual relationship with the workability and setting-time. A filament deposited successfully without blockage or fracture and that completes a length of 4500 mm was said to pass the extrudability criteria. The shear vane test was adopted to evaluate both the workability and open-time as it derives a relevant scientific rheological parameter and can evaluate the workability at various points in the production process, such as in the mixer or container. The acceptable workability limit that maintained extrudability was found to be within a shear strength of 0.3-0.9 KPa. The buildability was evaluated by counting the number of layers that could be stacked above each other without any noticeable deformation or failure. Finally, the feasibility of the mix was evaluated by printing a 2 m long concrete bench consisting of 128 filaments of 6 m thickness. Malaeb et al. [34] followed a similar procedure as the previous study and developed a printable mixture with a compressive strength of 42 MPa. In this study, the slump flow test was adopted to measure the flowability of the mix, and the open-time was calculated by getting the flowability over different time intervals. Finally, the optimal mix was evaluated by printing a wall that is 77 cm, 10 cm, and 10 cm, in length, width, and height, respectively. This highlights that the key properties of the fresh printing concrete are the extrudability, workability, setting-time and buildability.

Perrot et al. [35] followed a different approach and developed a model that predicts the structure failure during the printing process. The model was based on the idea that the first deposited layer should have sufficient mechanical strength to withstand the load caused by the upper layers. The mechanical strength of the first layer is related to the cement-based material yield stress, and the load caused on the first layer by the upper layers is linked to the building rate at which the layers are printed. The yield stress of the first layer was measured using an Anton Paar Rheolab

QC rheometer equipped with suitable vane geometry and the vertical stress acting on the first layer was simulated by placing a cylindrical sample with a 60 mm diameter and 35 mm height between two plates with the upper plate being loaded at 1.5 N increments. Different time gaps between the layers were experimented ranging from 11s to 60s with an average building rate ranging from 1.1 to 6 m/h. A LVDT-type displacement transducer was used to find the upper plate displacement with respect to time to detect the failure. The sample, which had a time gap of 60s and 1.1 m/h building rate did not experience any failure and the remaining samples with lower time gaps and higher building rate all failed due to insufficient mechanical strength. To further proceed and develop the model the critical stress of the first layer, which is linearly related to the yield stress, was determined and compared with the vertical stress. The study was able to predict the time at which failure will occur by plotting the development of the vertical and critical stress with time. The failure time occurred when the critical stress intersected with the vertical stress. The failure time predicted was in agreement with the experimental results conducted on the cylindrical sample. In addition, an analytical prediction of failure time (t_f) was also made using the linear evolution of yield stress. The experimental results were highly correlated with the analytical prediction t_f value except for the smallest building rate of 1.1 m/s. A 70 mm diameter column was printed with building rates of 1.1 to 6.2 m/h to validate the model and it was found out that the predicted failure times were in agreement with the experimental results. This highlighted the importance of studying the mechanical strength of the first deposited layer, which in turn helps in finding the optimal building rate at which the structure should be built to avoid failure.

Kazemian et al. [36] proposed and examined a framework for the evaluation of fresh printing concrete. The framework consists of a trial mixture which first has to be designed, then three factors, known as the print quality, shape stability, and printability window have to be tested, and finally the mixture has to be tested on a full-size printer in a similar environment as the intended project. A laboratory concrete printer similar to the Contour Crafting, which prints 38.1 mm by 25.4 mm layers, was developed in order to evaluate the proposed framework. The study developed four mixes, the first mix was a control mix, the second, third, and forth incorporated Silica Fume (SF), fiber and Nano-clay, respectively to evaluate its effect on the fresh properties of printing concrete. The first factor in the framework, which is the print quality, is related to the properties of the printed layer. For the print quality to be accepted three requirements should be satisfied which are 1) the printed layer should be free of any surface defects or discontinuities, 2) the layer edges must be squared not rounded, and 3) dimension conformity and consistency must be satisfied. This criterion is similar to the extrudability criterion defined by Le. et al. [25]. The second criteria in the framework, which is the shape stability refers to the ability of the layer to resist deformation under its self-weight, pressure from upper layers, and extrusion pressure. To know the time gap between the layers, the construction of a 108 square-meter one-story building was considered, and the nozzle traveling distance was found out to be 67 mm with a 60 mm/s building speed, therefore a time gap of 19 min was calculated. The shape stability was studied for time gaps of 0 and 19 min. Two tests known as the layer settlement and cylinder stability were proposed to evaluate the shape stability. The layer settlement was tested by a camera that was placed in front of two printed layers with time gaps of 0 and 19 min. The captured images were analyzed on a java-based image-processing program, which measured the layer settlement. At a time gap of zero, the control mix collapsed, whereas, the mix incorporating Nano-clay exhibited the lowest settlement. Conversely, all mixes incorporating SF, fiber and Nano-clay had zero settlement at 19 min time gap. The other test proposed for the shape stability is the cylinder stability and could be used instead of the layer settlement. In the cylinder stability test, concrete is filled in two layers in the cylinder shell, and each layer is compacted 15 times with a rod, then the cylinder shells are removed, and any settlement due to self-weight is measured, finally, a 5.5 kg (4.77 KPa) is applied to the sample and the deformation is recorded. The results of this test were similar to the layer settlement test as the mix incorporating Nano-clay showed the lowest deformation. The third factor in the framework is the printability window, which refers to the time at which the concrete can be extruded out of the nozzle with acceptable quality. Two limits were introduced under the printability window, which are the printability limit and blockage limit. The printability limit is defined as the time at which the printed layer is affected, and the blockage limit is the time when concrete cannot be extruded anymore out of the nozzle. The printability limit was tested by printing a layer every 5 min after 20 min of the initial contact with cement and water, and the blockage limit was recorded when concrete could not be printed anymore. Accelerator ($CaCl_2$) dosages of 1, 2, and

3% were added to the control mix and the initial setting time of the concrete was measured by concrete penetrometer as per ASTM C403 standard. In addition, the change of workability with time was measured by performing the flow test at different time intervals. The printability limit was found to occur before the initial setting time of the concrete, and it was therefore concluded by this study that the conventional test methods for setting time and flowability cannot replace the printability and blockage limit which are both dependent on the extrusion mechanism of the concrete printer itself.

From the previous studies, there is still no clear approach on how to investigate the fresh printing concrete properties. The two key properties that need to be addressed in the printing concrete are the extrudability and buildability and these two depend on the workability and setting time of the concrete. Other terms such as print quality, shape stability and structure stability were also defined; however, these terms are very similar to the extrudability and buildability and can fall under these criteria. Previously, in conventional concrete, the workability was defined as the ease at which the concrete mixture is transported, placed, compacted, and finished; however, this definition is not precise anymore for the printing concrete. The requirements that need to be satisfied by the workability are now different, as the workability should satisfy both the extrudability and buildability criteria of the printing concrete. In addition, new test methods to test the workability of the printing concrete should still be investigated. As for the buildability, comparing the yield stress of the first printed layer with the vertical stress acting above it will help in controlling the number of layers that could be printed above each other.

2.4.1.2. Rheology of Fresh Concrete. The science of studying the flow of matter and its deformation under shear stress is what is known as rheology. Amongst the famous models available to study the flow and fluidity of mortar is the Bingham model and can be described by the following equation:

$$\tau = \tau_y + \mu\gamma \tag{1}$$

Where τ is the shear stress, τ_y is the yield stress, μ is the viscosity, and γ is the shear rate.

The basic rheological parameters include, yield stress, viscosity, and thixotropy. The minimum stress required to initiate flow is the yield stress. Viscosity is the resistance of the material to change in shape or flow. The higher the viscosity, the more difficult will the flow be and vice versa. The loss of viscosity with time due to an applied stress is thixotropy, and can be defined as the energy required to breakdown a structure [37]. As shear stress is applied, the viscosity of a material decreases, and increases back again when at rest. Therefore, thixotropy is dependent on the change of viscosity with time. A material with high thixotropy indicates a high structural rebuilding rate. These properties are most commonly measured using concrete rheometers. A material with high yield stress, low viscosity, and high thixotropy are usually preferred for printing concrete. Even though very fast structuration rate, i.e. high thixotropy, is preferred for printing concrete, it has been found that high structuration rates may lead to the formation of cold joints and weak interfaces between the layers [38]. Thus, it is critical to monitor the thixotropy with the interlayer bond strength as there is a limit that should not be surpassed.

Two studies have evaluated the printing concrete based on its yield stress, viscosity, and thixotropy rheological properties[39, 40]. Zhang et al. [39] evaluated the effect of using different sand to cement ratio of 0.6, 0.8, 1.0, 1.2, and 1.5 on the fresh printing properties of concrete. From the study it was found that as the sand to binder ratio increases, the yield stress and viscosity increase, and the initial thixotropic value decreases. The change in yield stress, viscosity, and thixotropy with time was also measured for each mix. The thixotropy increased significantly with time, and the increase was highest for the mix with the highest sand to cement ratio. The yield stress and viscosity on the other hand were found to be not significantly affected by the time. The study confirmed that the ranges that maintained acceptable pumpability and extrudability were found to be 178.5-359.8 Pa for the yield stress, 3.8-4.5 Pa/s for the viscosity, and 6284.5 Pa/s for the thixotropy. Beyond these ranges the samples were either too wet or too stiff. A 192.5-269 mm initial spread diameter was found to be the optimal control range of flowability for the concrete to maintain its shape.

Panda et al. [40] investigated the effect of using one part geopolymers on the fresh concrete properties. Geopolymers are used as binders and are considered a more sustainable alternative for cement. They are produced by the chemical reaction of aluminosilicate materials such as fly ash and slag with sodium or potassium alkali activators. The amount of fly ash, slag, and alkali activator used will influence the properties of the final product of the reaction. In general, the carbon dioxide emissions of geopolymers are around 80% less as compared to cement. They are also better in terms of fire resistance and sulphate and acid attack. Other advantages include, high compressive strength, controlled rapid setting and hardening, and the utilization of waste materials as raw materials. Panda et al. [40] reported that an increase in the GGBS content of the geopolymer led to an increase in both the yield stress and viscosity, and a decrease in the setting time. Also, the yield stress increased with the increase in activator dosage. Regardless of the GGBS and activator content, the viscosity of the geopolymers was less than 10 Pa/s under a high shear stress which is very beneficial for 3D printing concrete. Similar to the yield stress and viscosity, the thixotropy was also increased with the increase in GGBS content. The mixes had a viscosity recovery of 70 to 80% of their original viscosity within a 60s-time interval. Therefore, the time selected to deposit the second layer was 60s to avoid the deformation of the first layer.

In general, when a material is extruded through a nozzle it exhibits a yield stress, initial elastic shear modulus, and initial critical shear strain. The yield stress and shear modulus increase with time whereas the shear strain decreases with time at rest. This causes the material not only to be stronger (high yield stress), but also more rigid (higher elastic shear modulus). The yield stress and the elastic shear modulus are the result of colloidal attractive forces that causes the cement particles to flocculate and result in a network of interacting particles. Prior to the deposition of the concrete from the nozzle, the concrete should have a yield stress and viscosity that is low as possible to facilitate the pumping. The initial yield stress and viscosity can be assessed by using rheometers. Most of the times the consistency reached by the printing concrete after several minutes may reach the upper limit of most of the standard rheometers, and thus, not measuring the equivalent yield stress and viscosity. The filament must have an initial yield stress after deposition for its shape to be controlled. The yield stress must sustain the gravity stresses that are caused by the deposition itself, and therefore, the yield stress must be in the order of ρgho [41]. Where, ρ, g, and ho are the density, gravity, and height of the filament.

From the previous discussion, the importance of the rheological properties for printing concrete was highlighted. For printing concrete application, it is vital to study properties such as the yield stress, viscosity, and thixotropy to be able to express the workability that will satisfy both the extrudability and buildability criteria. Hu [42] have shown that a relationship exists between the flow table test and rheological parameters (yield stress and viscosity) at very low amount of aggregates. Ames [37] on the other hand investigated the correlation between the rheological properties and the flow table test at a 75 min time scale for different mixtures. The mixtures composed of different replacements of clay (actigel, high reactivity metakolin, and ground clay brick). Different types of cement (ashgrove type I, lafarge type I/II, high alkali, and type IV) were used to evaluate its effect. The flow percent obtained from the mortar test result may be an indication of the structural rebuilding rate. From the research, it was observed that a relatively strong correlation exists between the flow percent decrease with time and the structural rebuilding rate. Up to the authors knowledge, the relationship between the rheological parameters and the mortar flow test have not yet been studied for the printing concrete. Similar to the slump test, the mortar flow test is easier to be applied on site for its ease of use and immediate results. It would be interesting to assess the applicability of the mortar flow test for printing concrete and correlate the corresponding results with the rheological properties.

2.4.1.3. Interlayer bond strength. The interlayer strength between the bond layers is one of the main limitations of the printing concrete when compared to the cast concrete. Potential flaws may occur between printed layers which induces stress concentrations. In conventional concrete, the bond strength between the existing concrete, and the new concrete, is affected by two factors, which are the surface and moisture of the printing concrete [43]. There are some controversies regarding the amount of moisture that should be present in the existing concrete to ensure sufficient bonding. It has been stated that free water on existing concrete reduces the bond strength, whereas, it has been stated by others that the moisture content does not affect the bond strength and that the bond is best at saturated surface dry condition (SSD) [44, 45]. As for the printing concrete, the concrete is still fresh, and therefore, it is critical to study the factors that influence the bond strength between the fresh layers. The viscosity is the main factor that affects the bonding and that is dependent on time.

Therefore, time is a critical parameter to be monitored. The time between the layers have to be selected such that 1) it is long enough to ensure that the filament has gained the required strength, and 2) it is short enough to ensure sufficient bonding.

Le et al. [46] studied the effect of time on the bond strength where the direct tension test was applied. It was found out that as the delay time increases, the bond strength, decreases which is logical as the viscosity of the fresh concrete decreases. Sanjayan et al. [47] studied the effect of moisture on the bond strength. The mix consisted of a sand to cement ratio of 1.5 and a water to cement ratio of 0.38. Two layers with dimensions of 250(L)x25(W)x15(H) mm were extruded with three delay times of 10, 20, and 30 min. The interlayer strength was tested by applying the uniaxial tension test shown in Figure 2.9. Specimens of 50x25x30 mm were sawn from the 250x25x15 mm printed samples. The test results showed that all the specimens failed at the interface between the first and second layer. The interlayer strength was observed to be higher for the 10 and 30 min as compared to the 20 min. It was hypothesized by the study, that as the concrete exits the nozzle there is a significant amount of moisture on the surface due to the extrusion process. After the layer is exposed to air, the water evaporates, leaving the surface dry and rigid. However, further increase in delay time results in additional moisture to be brought to the surface due to bleeding (30min). Two tests were further conducted to evaluate this hypothesis which are the surface moisture and the bleeding rate. The moisture content was checked for printed specimens as well as cast specimens at 10, 20, and 30 min. A paper towel was weighed and placed on the specimens and the weight was recorded to determine the surface moisture. For the cast specimen it was found out that the surface moisture increases with time, whereas, for the print specimen the surface moisture was highest for both the 10 and 30 min. This is the same trend observed by the uniaxial tension test. The bleeding rate was determined for the print specimens and the results showed that there was no bleeding from 0 to 20 min, and from 20 to 30 min there was sudden increase in the bleeding rate. The higher surface moisture at 0 min is due to the high pressure caused during extrusion which causes pressurized bleeding. From this study it was observed that the moisture level is affected by several parameters such as the moisture ejected during extrusion, bleeding and evaporation rate.

This shows that the interlayer strength is a function of many parameters and is dependent on the extrusion mechanism as well as the material constituents and proportions. The extrusion rate affects the amount of surface moisture present on the surface which indirectly affect the evaporation rate and bleeding rate which are dependent on the environment atmosphere. The sand to binder and water to binder ratios are also factors that affect the bond strength. These two ratios affect the structuration rebuilding rate of the paste. The lower the water to binder ratio and the higher the sand to binder ratio increase the structuration rebuilding rate (thixotropy). Even though high thixotropy is preferred in printing concrete, it has been observed recently, that this may lead to cold joints and weak interfaces [38]. Further research at this stage is still required to assess the parameters affecting the bond strength of the printed layers.

Figure 2.10: Test Setup of inter-layer strength measurement [47]

2.4.2. Mechanical properties and shrinkage control. As the 3D printing technology have already been used in practice, it is vital to study the mechanical properties of 3D printed components. Properties such as the density, compressive strength, flexural strength, tensile bond strength, elastic modulus, and drying shrinkage are currently being investigated. It was observed by several studies that anisotropy is most likely to occur in the layered structure of any freeform component [5, 39, 46, 48]. Anisotropy is when a material has different properties when measured in different directions. This likely occurs as a result of the bond between the filaments and between the layers [22, 46]. It is crucial to study the interfacial properties to assess the overall performance of the structure. Le et al. [46] reported that a correctly executed extrusion process may introduce little anisotropy in terms of compressive strength. Circular filaments with insufficient flow may result in air cavities which in turn affects the mechanical properties. Square and rectangular filaments with sufficient flow capacity may result in solid sections and better properties [22]. Zhang et al. [39] reported that the longitudinal (z) direction showed the highest compressive strength, followed by the y and x directions. Also, the increase in sand to binder ratio from 1.0 to 1.2 was found to increase the compressive strength in the three loading directions. The printing performance, print path, printing speed, and nozzle shape and size are all factors that affect anisotropy. Research on studying the extent of anisotropy is still ongoing.

Nerella et al. [49] reported that at the age of 21 days, the printed specimens had compressive strengths higher than 80 MPa. Also, the printed specimens on average had 10.5 and 12.8% higher compressive and flexural strengths as compared to the cast specimens. The use of 52.5 grade rapid setting cement contributed primarily to achieving high early strengths. Le et al. [25] incorporated 1.2 kg/m^3 micro polypropylene fibers which resulted in 20, 80, and 110 MPa compressive strengths at the age of 1, 7, and 28 days. 3D printed structures are printed with no formwork, this may increase the water evaporation process, and shrinkage may occur as a result. Shrinkage will affect both the dimensional accuracy and stability of the structure; therefore, it is essential for 3D printed concrete to have low shrinkage properties to compensate for this. The use of shrinkage reducing admixture (SRA) is usually utilized to reduce the shrinkage effect by lowering the surface tension induced by water evaporation [50]. Other solutions that may help control the shrinkage effect include reducing w/c ratio, increasing sand to binder ratio, and adding fibers.

Table 1.1: Summary of fresh printing concrete evaluation from the literature

Study	Printing Details	Materials Used	Fresh Properties Investigated	Evaluation Methods and Criteria	Conclusion
Le el al. [25]	• 5.4X4.4X5.4 m. • circular 9 mm diameter nozzle.	Cement, FA, SF, polypropylene micro fibers of l/d of 12/0.18mm, retarders, and accelerators.	Extrudability	Evaluated as "Yes" or "No" the former being when a length of 4500 is deposited without blockage.	• Shear strength that maintained the extrudability lied within a range of 0.3-0.9 kPa. • Optimal shear strength for buildability 0.55 kPa. • Up to 15 layers were reached for group 1 filaments which consisted of 1 bottom layer. • Open-time: 100 min
			Buildability	Quantified the number of filament layers that could be built up without any noticeable deformation	
			Workability	Determined the shear strength by determining the torque according to BS 1377-9:1990 using the Shear Vane test apparatus. A 90 mm diameter shear vane was used.	
			Open-time	Monitored the workability that maintained extrudability over a time period of 15 min using the Shear Vane test.	
Malaeb et al. [34]	• Circular 20 mm diameter nozzle. • printing speed 18.76	Cement, superplasticizer, viscocrete, retarders, and	Extrudability	Evaluated visually when concrete was free of any separation and cracks.	• Flowability should be within 1.0-2.0 cm/s to meet the extrudability and buildability requirement.

	cm/sec, and extrusion rate 0.09 L/sec.	accelerators.	Buildability	Quantified the numbers of layers that could be built up without deformation.	
			Flowability	Adopted the Slump-Flow test, and the spread diameter was measured over time.	
			Open-time	Monitored the flow of concrete over specific time intervals.	
Perrot et al. [35]	-	Cement, kaolin, limestone, and polycarboxylate type powder based SP.	Yield stress	Measured for first layer using Anton Paar Rheolab QC rheometer equipped with suitable vane geometry.	• A prediction model was developed which finds the relationship between the yield stress and vertical stress. • The model predicts the time at which the layers collapse.
			Structural build-up	Measuring the vertical stress acting above the first layer. Vertical stress was simulated by adding a cylindrical sample between two plates, and loading the upper plate at 1.5 N increments.	
Kazemian et al. [36]	• 38.1X25.4 mm. • printing speed of 60 mm/s.	Cement, SF, fibers, and nano clay.	Print quality	Evaluated as "Yes" or "No" when the following are satisfied: 1) the printed layer should be free of any surface defects or discontinuities, 2) the layer edges must be squared not rounded, and 3) dimension conformity and consistency must be satisfied.	• At 0 min time gap between the layers, nano clay exhibited the lowest settlement when compared to mixes containing only cement, SF, or Fibers. • Cylinder settlement test was found to be a satisfactory test for the shape stability and can

			Shape stability	Evaluated using two tests: 1) layer settlement, and 2) cylinder stability. • Layer settlement: 2 layers are extruded above each other and a camera was used to determine the settlement using Java. • Cylinder settlement: concrete is filled in two layers in a cylindrical mold which is then compacted 15 times. Cylinder is removed and settlement is recorded.	replace layer settlement. • Setting-time cannot replace times such as the printability and blockage limit.
			Printability limit	Tested every 5 minutes until the print quality is not satisfied.	
			Blockage limit	Tested every 5 minutes until blockage occur.	
Zhang et al. [39]	• 3.8X2.7X2.8 m. • Circular nozzle with diameter of 20 mm. • Printing rate 133.33 mm/s.	Cement, nano clay, SF, polycarboxylate and based high range water reducer.	Workability	Evaluated using drop table test.	• Workability/flowability right after mixing to ensure good extrudability was in the range of 192.5-294 mm. • The concrete rheometer did not measure the thixotropy of the mixes with a/b ratio higher than 1.2 after 15 min as the mixes were too stiff. • Optimal ranges of yield stress, viscosity, and thixotropy are 178.5-359.8 Pa, 3.8-4.5 Pa.s, and 6284.5 Pa/s. Beyond these ranges, the concrete is either too wet or too stiff.
			Yield stress, Viscosity and Thixotropy	Evaluated using a concrete rheometer. Concrete was regarded as a Bingham Fluid ($\tau = \tau y + \mu\gamma$).	

Panda et al. [40]	• Rectangular nozzle of 40X10 mm dimension. • Printing speed 90 mm/s.	One part geopolymers composed of aluminosilicate materials (GGBS/FA), and alkaline activator (potassium silicate and potassium hydroxide).	Yield stress	Adopted the Stress Growth test were deformation was applied at a constant shear rate of 0.1 s^{-1} .	• The use of geopolymers in concrete led to having concrete with high yield stress, low viscosity, and high thixotropy which is beneficial for 3D printing concrete. • The use of geopolymers led all mixes to have low viscosity under high shear stress (<10 Pa.s) which is beneficial for pumping. • All mixes had a viscosity recovery of 70-80 % of their original viscosity during 60 sec. Therefore, the time between the layers was selected to be 60 sec so that the previous layer has already gained some of its stiffness.
			Thixotropy	Measured using a structural parameter (λ) which is calculated by $\lambda = \frac{\tau o - \tau e}{\tau e}$. Where τo and τe are the intial shear stress and equilibrium shear sress, The higher the λ, the higher the thixotropy.	
			Viscosity recovery	Simulated at three different shear rates of 0.01 s^{-1} for 60 sec, 300 s^{-1} for 30 sec, and 0.01 s^{-1}.	
Ma et al. [51]	• Steel fram size 0.5X0.39X1.1 m. • Plat form 40X20 cm. • Rectangular nozzle of 8X30 mm dimension. • Printing speed 75 mm/sec.	Rapid hardening cement (22.0 MPa) FA, and SF. Copper tailing used as a partial replacement for sand river fine aggregates. Polypropylene fibers	Extrudability	Evaluated as "Yes" or "No" when a total continuous length of 2000 mm is deposited in eight turn processes without separation, liquid drainage, or blockage.	• The shape retention decreases with the increase in copper tailing replacement. • Open-time was determined to be 70 min. • Flowability (slump and jumping table) increases as the tailing content increases. • Slump and spreading diameter range to maintain printability were found to be 88-32 mm, and 175-210 mm. • The V-funnel was found to be a
			Buildabilitiy	• Designed to stack 20 layers of extruded filaments with a 250 mm length with a time gap of 10 min to avoid cold joints. • The average vertical strain of each printed layer is measured to describe the shape retention.	

			Open-time	• Measured as the time that maintain acceptable extrudability, and the flowability and penetration are monitored along with the open-time.	good indication for the viscosity. From the test, it was found out that to some extent the increase in trailing content increases the binding effect of cementitious materials which therefore enhance the binding between the layers. • The penetration resistance increased with the increase in tailing replacement. When the penetration resistance increased beyond 40, the filaments no longer satisfied the extrudability criteria.
			Flowability	• Measured using three tests: 1) Slump test GB/T14,902-2012, 2) V-funnel test JBJ/T283-2012, and 3) jumping table test GB/T 2419-2005. • Slump dimensions: 100, 50, and 150 mm at base, top, and height. • In the jumping table, the flowability is measured as the average diameter in two perpendicular dimensions after 25 drops.	
			Structural build-up	• Adopted the Penetration Resistance Method GB/T 50,080-2002 to access the structural build up behavior of cementitious materials Needle of 100 mm² is pressed to a depth of 25±2 mm. A spring connected to needle measures the penetration accordingly	

Chapter 3. Methodology

The methodology of this study is mainly divided into three main stages which are the extensive literature, materials and mix proportions and experimental program. Each stage along with the tasks involved are described below.

3.1. Extensive Literature

The first task was to gather information from secondary sources to collect the state-of-art knowledge of the 3D printing technology and to know the theoretical and methodological contributions in this area. Information on the 3D printing technology, the famous techniques available, printed structures, materials used, and properties investigated have already been gathered. This stage have helped in knowing what is yet to be investigated in this area and identifying the tasks that will be involved in the second stage of the methodology which is the experimental program.

3.2. Materials and Mix Proportions

As discussed, there are certain objectives that need to be achieved by the printing concrete. The printing concrete must be extrudable, flowable, and buildable with good mechanical properties and low shrinkage. The materials used in this study include, dune sand, crushed sand, ordinary portland cement (OPC), ground granulated blast furnace (GGBS), and silica fume (SF). The specific gravity and water absorption of the used materials are given in Table 3.1. The maximum aggregate size of the dune and crushed sand is 4.75 mm, and the fineness modulus is 0.48 and 3.2; respectively. The materials used are all shown in Figure 3.1.

Table 3.1: Physical properties of fine aggregates

Materials	**Specific Gravity**	**Water Absorption (%)**
Dune sand	2.58	2.20
Crushed sand	2.57	1.00
OPC	3.14	NA
SF	2.20	NA
GGBS	2.91	NA

Phase 1- Two groups of mixes (Group I and Group II) were first prepared to evaluate the effect of using different materials on the extrudability. Both groups consisted of 4 mixes; however, Group I mixes were prepared with dune sand only,

and Group II mixes were prepared with a blend of both dune and crushed sand. The four mixes of the two groups consisted of a mix pepared with OPC only (control mix), OPC and GGBS, OPC and SF, and OPC, GGBS and SF combined. A commercially available superplasticizer (MasterGlenium SKY 504) and viscocity modifier admixer (VMA) (MasterMatrix 110) were used in all mixes. All mixes were prepared with a constant water to binder (*w/b*) ratio of 0.26. Along with the extrudability, the compressive strengths of the two groups were also computed at 3 and 28 days. Note that the reference of the two groups of mixes are given such that the first one or two letters refer to the type of sand used either dune sand (D), or dune and crushed sand combined (DC), these letters are then followed by a hyphen to indicate the type of binder used in the mix. CM for control mix consisting of portland cement only, GB for ground granulated blast furnace, SF for silica fume, and GBSF for GGBS and SF combined. For instance, DC-GBSF refers to the Group II mix which has fine aggregates consisting of dune and crushed sand and binding material of OPC, GGBS, and SF combined. The mixes of the two groups are shown in the Figure 3.2.

Figure 3.1: Materials used in the mixes

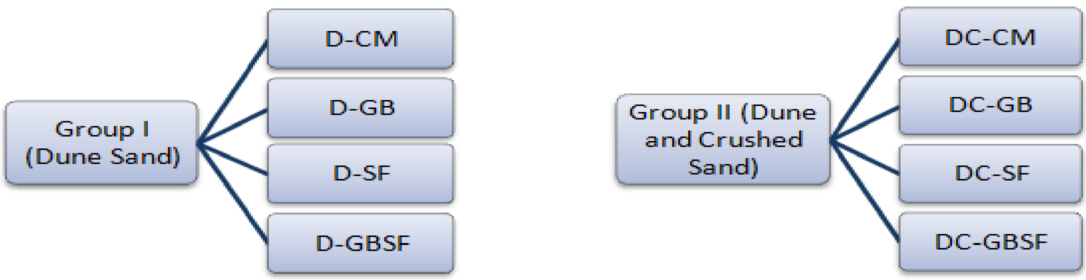

Figure 3.2: Phase 1 mixes

Phase 2- Based on the extrudability and compressive strength results of the 8 mixes, the optimum mix of the two groups was selected and subsequently used to investigate the other fresh properties. The DC-GBSF with an aggregate to binder (*a/b*) ratio of 1.2 was the optimum mix selected from Phase 1. Another two mixes of the same mix were developed with an *a/b* ratio of 1.5 and 1.8. These mixes were developed to assess the effect of different aggregate to binder ratios on the extrudability, setting-time, workability, open-time, buildability, and compressive strength. The test methods used to evaluate each of these properties are discussed in the following subsections. The mixes of phase 2 are shown in the Figure 3.3.

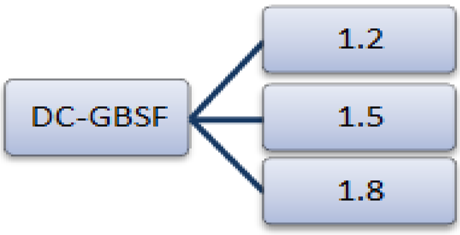

Figure 3.3: Phase 2 mixes

3.3. Experimental Program

This stage provides information on the mixing and printing procedure as well as the tests conducted to evaluate the extrudability, open-time, setting-time, workability, buildability, and compressive strength.

3.3.2. Mixing and Printing Procedure. In phase 1 evaluation, each mix of the 8 mixes had to be repeated several times to obtain the best extrudability results. Therefore, it was rational to start by mixing a small volume of concrete until the extrudability is achieved. The Hobart mixer demonstrated in Figure 3.4 was the type of mixer selected to be used during phase 1 evalution. This was mainly because the mixer allows for the mixing of a concrete volume that would satisfy both the volume required for the extrudability and compressive strength, and allows for the usage of different mixing speeds of 140 ± 5 rpm and 285 ± 10 rpm. The Hobart mixer have proven to be very efficient for mixing concrete with a w/b ratio of 0.26. Sanjayan et al. [47] have also used the Hobart mixer for mixing printing concrete to assess the interlayer strength and the hardened printed concrete properties.

In phase 2 evaluation, the optimum mix (CS-GBSF) was selected from phase 1 and was developed with three different *a/b* ratios of 1.2, 1.5, and 1.8. The Hobart Mixer was again used for mixing, and the extrudability, setting time, buildability, and compressive strength were evaluated. After the extrudability and buildability were satisfied it was necessary to mix larger volume of concrete to evaluate the remaining fresh properties of the concrete which are the workability and open-time. The Hobart Mixer was no longer applicable to be used as now the volume of concrete had increased and thus the normal concrete mixer demonstrated in Figure 3.4 was used. This type of concete mixer was not very efficient for mixing concrete with 0.26 *w/b* ratio. It is important to note, that in order to achieve the same properties of mixes mixed with the Hobart Mixer, the mixing time had to be significanlty increased. This may clarify why the concrete mixes developed for different 3D printers may have to be readjusted. The effect of mixing is further explained in the Results and Discussion chapter.

Figure 3.4: Types of Mixers Used

All the mixes prepared using the Hobart Mixer were first allowed to rotate with a low speed of 140 ± 10 rpm for 1 minute and then the mixer was turned on at a medium speed of 285 ± 10 rpm for 2-3 minutes. After approximately 4 minutes, the VMA dosage was added and the mixer was allowed to rotate at a low speed for 1 minute. As for the normal concrete mixer, after the dune and crushed sand were added to the mixer, water was first added to the fine aggregates to account for the water absorption. The mixer was then rotated for 1-3 minutes, followed by the addition of the rest of the materials. The water was added roughly in around two halves, the first half added to the mix did not contain any superplasticizer whereas the second half contained all the superplasticizer dosage. After the lumps were broken down and the mix was observed to be consistent, the VMA dosage was added. The normal concrete mixer had a speed of 17.5 rpm and the mixing time was approximately 40 minutes. Note that while mixing the mixer had to be tilted several times to make sure that the water, superplasticizer, and VMA had reached all the particles of the mix.

A custom-made 3D printer nozzle was manufactured to simulate extrusion-based 3D printing process. A piston type extruder was used and moderate external vibration was applied to ensure that the mixture is adequately compacted inside the extruder. Two nozzles were used, a circle nozzle with diameter of 17 mm and a square nozzle with dimensions of 20x20 mm. Figure 3.5 demonstrates the square nozzle extruder.

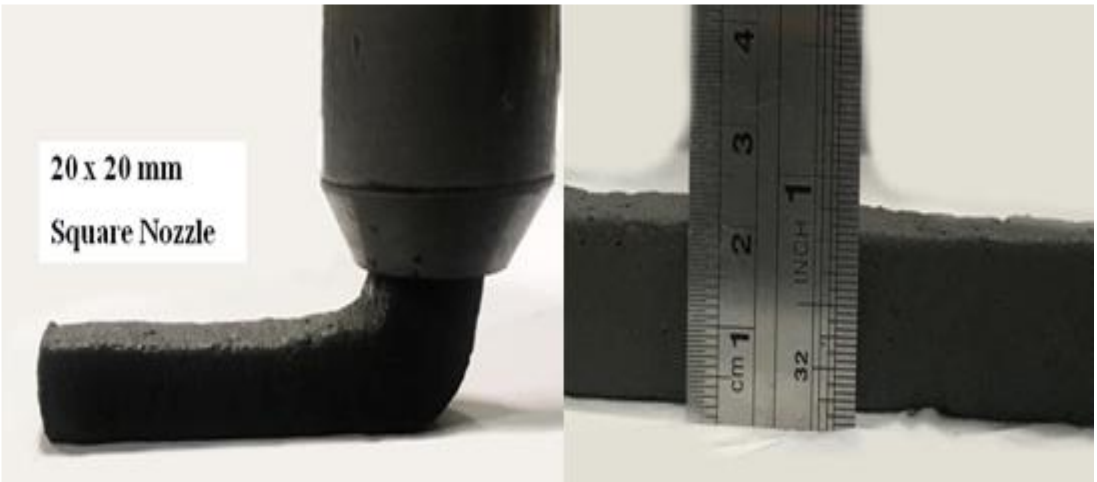

Figure 3.5: Custom made nozzle

3.3.3. Tests Conducted for Evaluation. The tests conducted in phase 1 and phase 2 are all presented below. Figure 3.6 shows a summary of the tests conducted and type of mixer used in each phase.

3.3.3.1. *Extrudability.* The first property to be investigated for the printing concrete is the extrudability which lies in a smooth grading of materials. Le et al. and Ma et al. [51] considered a target length for the extrudability; however, both Maeleb et al. and Kazemian et al. did not consider any target length when evaluating this characteristic and only focused on the shape of the filament itself as discussed above

[34, 36]. In this study for a mix to pass the extrudability criteria the following requirements have to be satisfied: First, the filament has to maintain the shape of the nozzle, and second, the filament has to be extruded continuously without any separation or blockage.

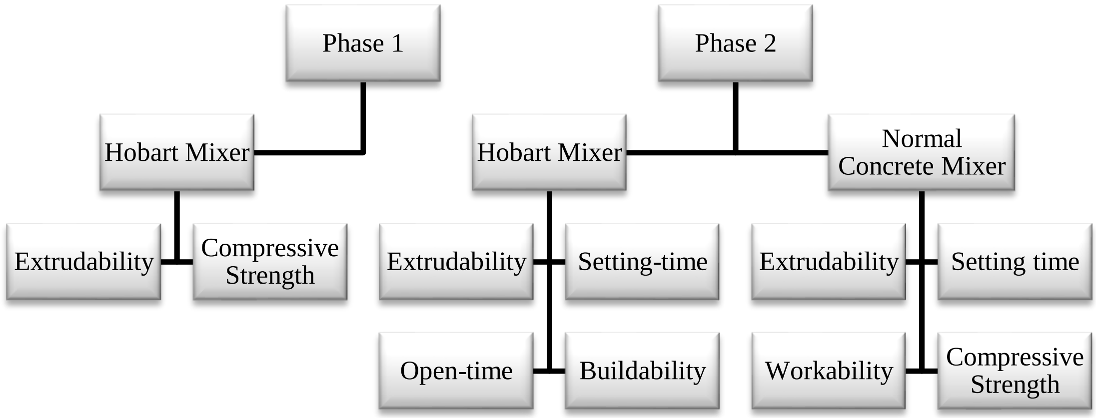

Figure 3.6: Summary of tests conducted in Phase 1 and Phase 2 evaluation

3.3.3.2. *Setting-time and Open time.* The setting-time was performed for the mixes evaluated in Phase 2, DC-GBSF, with *a/b* ratios of 1.2,1.5, and 1.8 by means of the Vicat Needle as per ASTM C191-04. The setting-time was determined using both the Hobart mixer and normal concrete mixer to ensure that both mixing methods led to the same initial and final setting-time. The open time, on the other hand, is the time at which the filaments are no longer satisfy the extrudability requirements. To determine the open time of the mixes, a filament was extruded every 15 minutes until the filaments could no longer extruded continuously. The time at which the filaments were not satisfactory was recorded as the open time.

3.3.3.3. *Workability.* The workability of the printing concrete should be within a range that maintains acceptable extrudability, flowability within the system, and buildability. As aforementioned, currently, in the literature, the rheological properties such as the yield strength, viscosity, and thixotropy, are being investigated to demonstrate the workability of the printing concrete [39-41]. Several studies have also conducted the slump flow test at different time intervals. Methods such as the slump flow is preferred on sites for its ease of use and the immediate results. In this study two methods were adopted to study the workability of the printing concrete. The first test method involved performing the slump test. The slump cone originally has an internal diameter of 200 mm at the base and 100 mm at the top and a height of 300 mm. These dimensions are suitable for concrete that has an aggregate size of up to 37.5 mm. Since the concrete used in this study has a maximum aggregate size of 4.75 mm, and could be considered as mortar, two cones with different dimensions were initially proposed. The base and top diameter and the height of the proposed cones are 100, 50, and 150, and 25, 50, and 75 mm, respectively. The cone with the 100, 50, and 150 mm dimension shown in Figure 3.7 was first tried and was found to be satisfactory to perform the slump test. Ma et al. [51] proposed similar dimensions to test the slump of the mortar paste. Since this cone was satisfactory the cone with the other dimensions was not tried. The slump test was performed every 15 minutes until the concrete was no longer extrudable. The test gives an indication of the homogeneity, consistency and the buildability of the concrete mix.

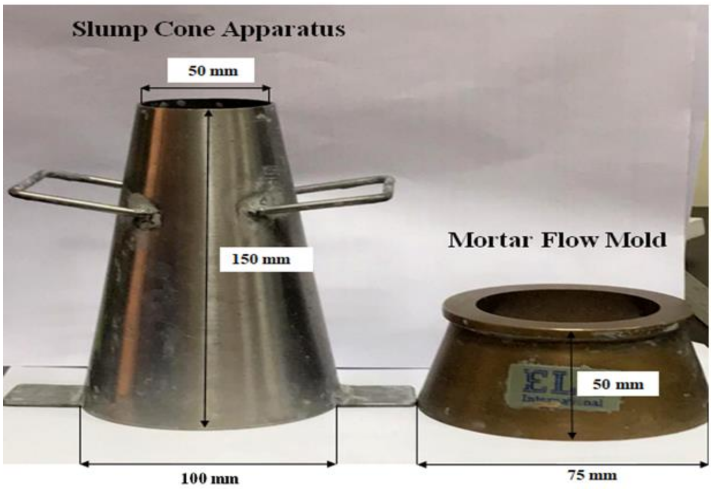

Figure 3.7: Slump and mortar mold

The second test method selected was the flow of mortar test which was performed as per ASTM C1437-01. The flowability was estimated based on the spread of mortar subjected to 25 drops in 15s of the flow table shown in Figure 3.8 (b). Using the caliper shown in Figure 3.8 which is specified in Specification C 230, the diameter is measured along the four lines scribed at the tabletop, and the flow is recorded as the total of the four readings. The flow test gives a better indication of the rheological properties of the concrete as compared to the slump test since it measures the resistance of the concrete to flow within a specific time, 15s in this case. As in the slump test, the flow test was performed every 15 minutes until the concrete was no longer extrudable.

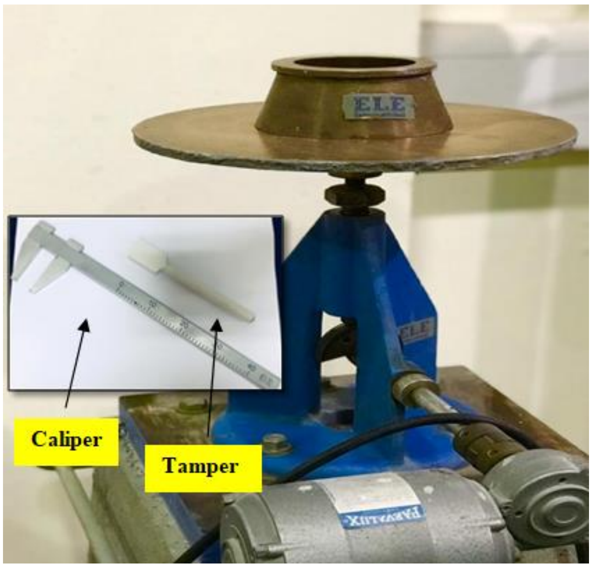

Figure 3.8: Mortar flow test apparatus

3.3.3.4. ***Buildability***. Buildability is the ability of the filaments to maintain their shape once extruded and bear the pressure that results from the upper layers. It is the vertical stacking of layers. The shape of the filament is one of the factors that affect buildability. Bos et al. [22] at TU/e are currently using square filaments with 40 x 10 mm dimension with no slump characteristics. These filaments were easier to stack than round filaments. Square filaments require the printer head to move in such a way to remain tangent to the tool path to avoid twisting of the filament in curves. In this study the buildability was measured by simply counting the number of layers that are stacked above each other.

3.3.4.5. ***Compressive Strength.*** The compressive strength was performed on all mixes in phases 1 and 2. In phase 1 the compressive strength of cast specimens of the two groups were tested at 3 days to have an indication of the concrete compressive strength while choosing the optimum mix. In phase 2, the compressive strength of both cast and printed specimens were performed mainly to evaluate the effect of the layering process on the concrete. The compressive strength was performed as per ASTM C109 on 50x50x50 mm specimens at both 3 and 28 days. The dimensions of the printed specimens were 60x60x60 mm which were prepared from a 160x60x60 mm printed samples, as shown in Figure 3.9. Printed specimens should be tested in three directions which are the perpendicular, lateral, and longitudinal directions, to determine the effect of the layering process on each direction. In this study, the specimens were only tested in the perpendicular direction. At least two specimens were tested in the perpendicular direction for each mix.

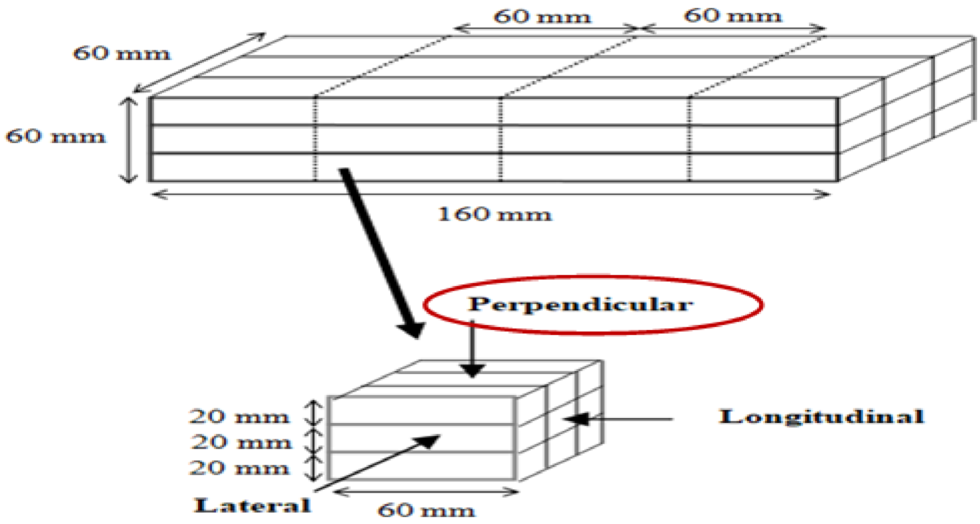

Figure 3.9: Cutting diagram and testing direction of printed concrete

Chapter 4. Results and Discussion

The results and discussion chapter is divided into two main sections which are Phase 1 and Phase 2 Evaluation. In phase 1, the extrudability and compressive strengths of Group I and Group II mixes are discussed. In phase 2, the extrudability, setting-time, open time, workability, buildability and compressive strength of the 1.2, 1.5, and 1.8 mixes are discussed.

4.1. Phase 1 Evaluation

4.1.1. Extrudability Evaluation. Group I - The extrudability of the D-CM and D-GGBS mixes was the most difficult to be adjusted. Several trials were done to adjust the extrudability of the control mix (D-CM) with aggregate to binder ratios ranging from 1.1 to 2.17. For the first trial the control mix had a *w/b* and *a/b* ratio of 0.26 and 1.3. This mix failed as it was too stiff to be extruded through the nozzle. Additional water and superplasticizer were added to try to adjust this mix; however, segregation occurred as a result and the mix became too flowable which led to blockage in the end. For this reason, the a/b ratio was altered several times to adjust the extrudability. The use of excessive dosages of either water or superplasticizer probably led the cohesiveness of the mix to drop which led to segregation and bleeding. The segregation of the 1.3 *a/b* ratio D-CM mix is shown in Figure 4.1.

Figure 4.1: Control mix segregation

The viscosity modifier admixture (VMA) was initially not used in the control mixes to prevent additional costs. Most of the mixes segregated when the water to binder ratio and superplasticizer dosages were increased; however, when VMA was used, segregation did not occur and the extrudability of almost all the mixes was achieved. It was thus concluded that the use of VMA is very critical to adjust the extrudability of the control mixes. The use of VMA reduces the risk of segregation by absorbing some of the free water in the system through chains of the water-soluble polymer which enhance the cohesiveness of the mix [52]. It also improves the pumpability of the mix. Figure 4.2 shows the extrudability of 1.3 *a/b* D-CM mix with and without the use of VMA. The mix with 1.2 a/b ratio was the easiest to adjust, and thus was selected to be the control mix of Group I. Several trials were performed on the 1.2 *a/b* mix to reach to the optimal dosage of superplasticizer and VMA which were found to be 0.46% by weight of the concrete mix.

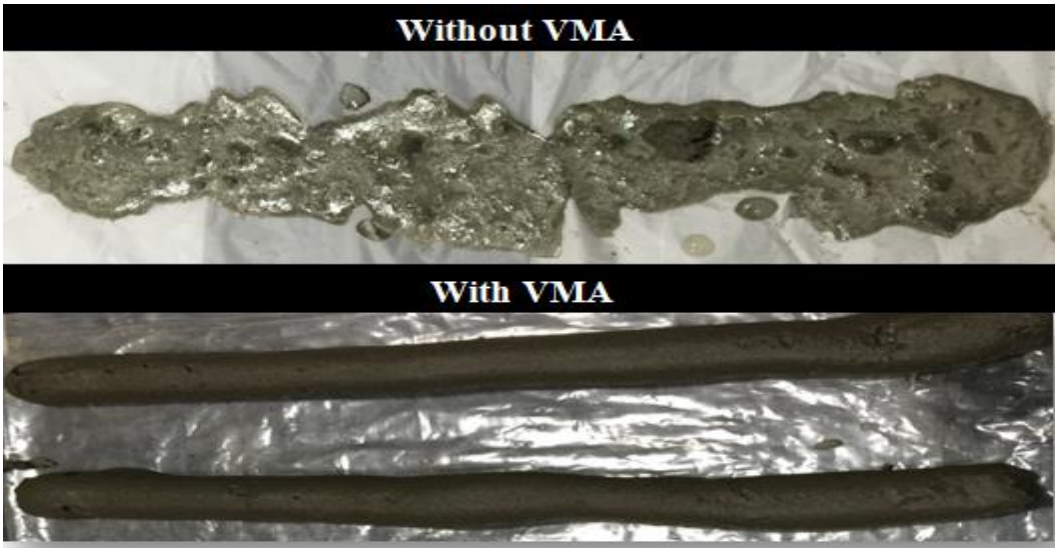

Figure 4.2: Control mix extrudability

After optimizing both the a/b ratio and additive dosages of the control mix, the remaining mixes of Group I were developed, which are D-GB, D-SF, and D-GBSF. The mixes were developed to have the same *w/b* ratio of 0.26 as the control mix. The D-GB mix was also difficult to extrude, and again, several trials had to be done to reach to the optimal dosage of superplasticizer and VMA. However, this mix was to an extent easier to extrude than the D-CM mix. The increased cohesiveness achieved by the addition of GGBS probably have improved the extrudability performance. The optimal dosages were found to be 0.38% by weight of the concrete mix. As observed the superplasticizer and VMA required were less than the control mix. This was expected as, unlike the cement, only little water gets absorbed by the GGBS due to the dense surface of the GGBS particles, and thus, this causes the concrete containing GGBS to have greater workability than the concrete made with cement only. Note that if the same amount of superplasticizer was used in the D-GB mix, the mix may have become too flowable, and this may have led to unacceptable extrudability. There are several reasons for blockage with the most common reason being when the mixing water in the concrete is not retained. If not enough water is added to either the control mix or the D-GGBS mix, the mix would be too stiff to extrude, and thus will require an increase in the flowability. The increase in flowability for extrusion can either be achieved by increasing the water to cement ratio or adding superplasticizer. This increase in flowability may either cause the mix to segregate or will result in filaments that are too wet to retain the shape of the nozzle. Therefore, the use of VMA is essential with the increase in w/b ratio or superplasticizer to adjust the viscosity of the mix and to account for the excessive water which may increase the chances of blockage.

As expected, the SF played a big role in enhancing the extrudability of the concrete. The D-SF was much easier to extrude than the D-CM and D-GB mixes. The use of SF is well known to increase the cohesiveness of the mixture which will in turn improve the pumpability of the concrete and enhance the extrudability. To obtain the combined benefit of each of the GGBS and SF, finally, a mix containing both materials was developed which is the D-GBSF. The extrudability of the D-CM, D-GB, and D-SF is presented in Figure 4.3.

Group II Mixes - Similar to Group I, the use of GGBS and SF had the same effect on Group II mixes. The DC-CM and DC-GB mixes were the most difficult mixes to adjust for extrusion as compared to the DC-SF and DC-GBSF. The use of crushed sand along with dune sand have facilitated the extrusion process for the four mixes as compared to the mixes of Group I. The addition of crushed sand probably has led to a smoother gradation curve which therefore resulted in a better extrusion performance. The sieve analysis results of the dune sand and crushed sand is shown in Figure 4.4 from which it is observed that the crushed sand had a smoother gradation curve than that of the dune sand which facilitated the extrusion process. All mixes incorporating both dune and crushed sand had higher flowability with a 0.26 *w/b* ratio than the mixes incorporating dune sand only. The increased flowability observed in these mixes were adjusted by the VMA dosage. The dune sand has a higher surface area as compared to the crushed sand as observed from the fineness modulus of both type of sands. Mixes with the same w/b ratios showed different flowability performance which might be attributed to the high surface area of the dune sand. The 0.26 *w/b* ratio could have been decreased for Group II mixes; however, it was kept constant in this study and the remaining mixes of Phase 2 were all developed with the same 0.26 *w/b* ratio. The optimum mix selected for Phase 2 evaluation is the DC-GBSF mix.

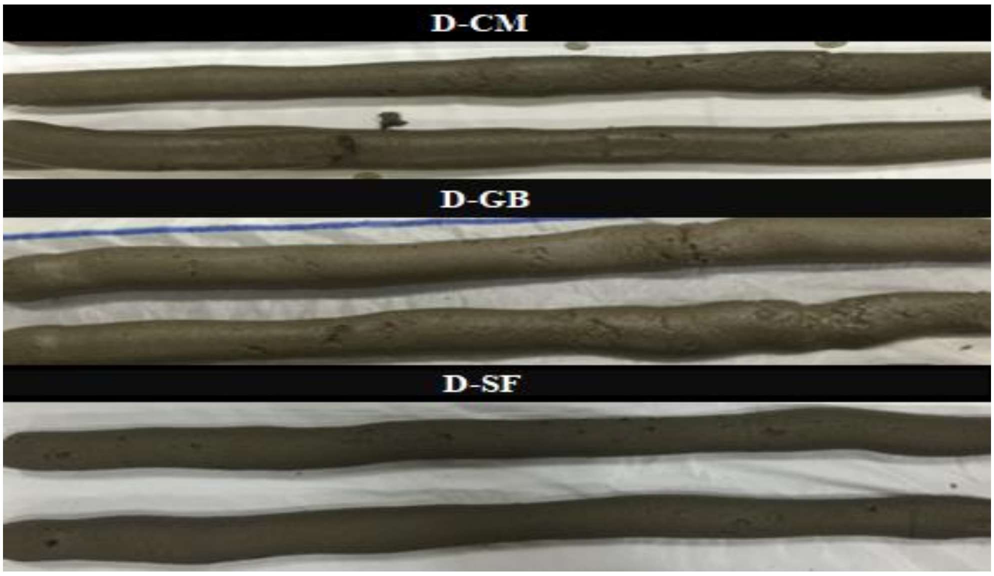

Figure 4.3: Extrudability of group I mixes

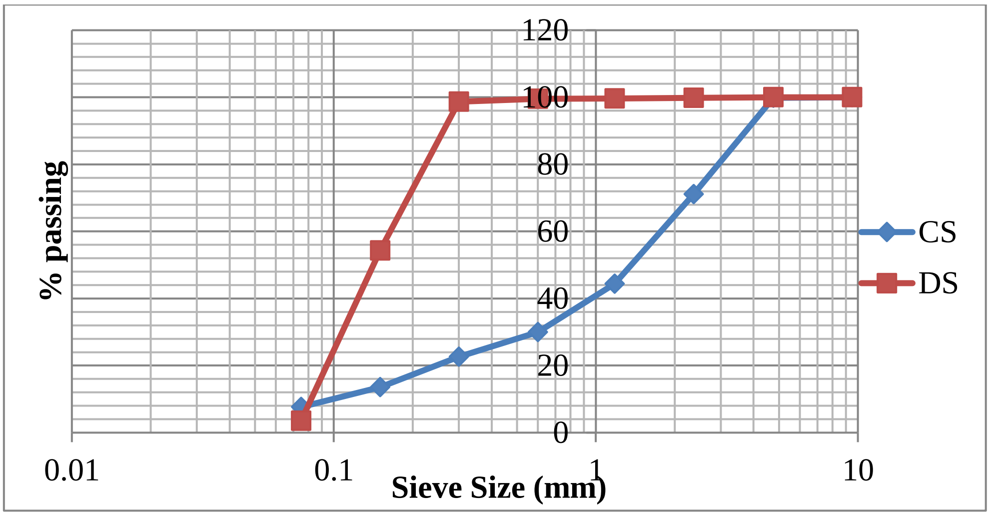

Figure 4.4: Sieve analysis for dune and crushed sand

4.1.2. Compressive Strength. The compressive strength for phase 1 mixes was tested mainly at 3 days to have an indication of the concrete strength while choosing the optimal mix for phase 2. Figure 4.5 shows the compressive strength at 3 days for both Group I and Group II mixes. When comparing the effect of the supplementary cementitious materials on concrete, it is observed, that the mixes incorporating GGBS had comparatively lower strengths to that of the control mixes. This was expected as GGBS mixes are known to have lower strengths at early ages, and greater strengths over the long term [53]. As for the mixes incorporating SF, the strengths were relatively higher than the mixes incorporating cement only or GGBS. SF increases the early age strength of concrete [54]. To date, the effect of SCM materials on concrete strength is well known, and the results of this study confirm with the literature findings. The use of crushed sand increased the strengths for all the four mixes and this can mainly be attributed to the crushed sand gradation curve. The DC-GBSF mix had the highest strength of 34 MPa at 3 days, and thus, was selected based on the extrudability and compressive strength results for phase 2 evaluation to test the fresh printing concrete properties.

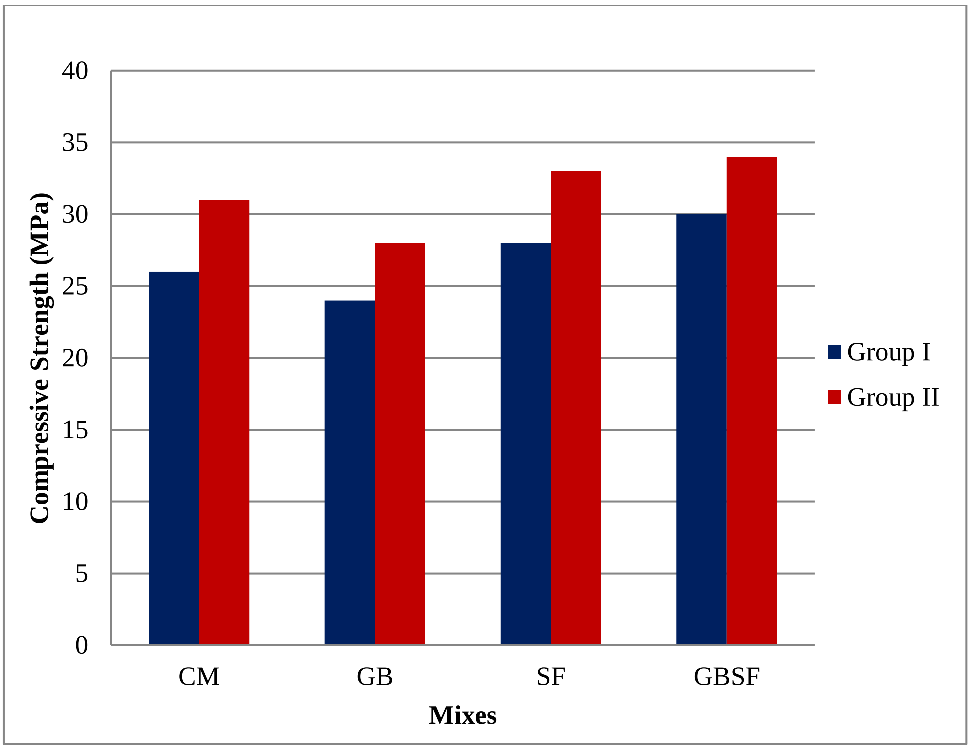

Figure 4.5: Compressive strength for Phase 1 mixes

4.2 Phase 2 Evaluation

As discussed in the chapter 3, three mixes with different *a/b* ratios (1.2,1.5 & 1.8) of the DC-GBSF mixes were developed. Two types of mixers were used for the evaluation which are the Hobart mixer and the normal mixing machine. The Hobart mixer was first used to test the extrudability, setting time, buildability and compressive strength. The normal mixing machine was mainly used to satisfy the volume amounts required for the workability evaluation.

4.2.1 Extrudability. The extrudability of the mixes were evaluated using both the Hobart Mixer and Normal Mixing Machine. Acceptable extrudability was observed for the *a/b* ratio 1.2, 1.5, and 1.8 mixes. All mixes showed good water retention properties and were delivered through the nozzle without any blockage or separation. Logically speaking the energy required to extrude each of the mixes should increase with the increase in aggregate to binder ratio. Initially, the energy required to extrude each of the three mixes was observed to be the same during the first couple of minutes. However, later a change in the rheology of the fresh concrete was anticipated and the rate of structuration of the mixes were different. In general, the extrudability is affected by the rate at which the fresh concrete is stiffening. As the mix gains strength, the energy or force required to extrude will increase. If this energy is kept constant, i.e. the extrusion rate, the filaments will no longer be extruded through the nozzle with time. The rate at which the mixes are stiffening can be observed from the setting-time results. Figure 4.6 shows the extrudability using the 20 x 20 mm square nozzle.

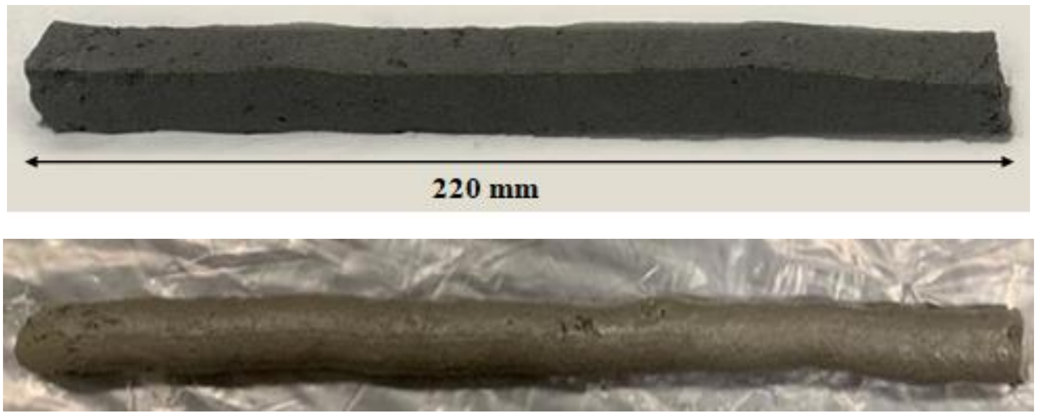

Figure 4.6: Extrudability using square and circular nozzle

4.2.2 Setting-time and open-time. The setting-time was evaluated using each of the two mixers. Figure 4.7 demonstrates the setting-time of the *a/b* ratio 1.2,1.5, and 1.8 mixes using the Hobart Mixer. The initial setting time (IST) is the time at which the paste starts losing its plasticity, whereas, the final setting time (FST) is the time at which the paste completely loses its plasticity. The IST and FST are recorded at a 25 and 0 mm penetration readings. Table 4.1 shows the IST and FST of the mixes. As observed from Figure 4.5 until approximately 75 minutes, all the mixes had a 40 mm penetration. After this point, the rate at which the mixes were stiffening was different as observed from the slopes of the curves. If the time gap between the layers exceeds the IST this may lead to the formation of cold joints between the layers. Cold joints are weak planes that occur when the two layers do not intermix. The FST on the other hand is essential to ensure normal hydration.

Table 4.1: Initial and final setting time of a/b ratio 1.2, 1.5 and 1.8 mixes

	1.2	**1.5**	**1.8**
IST (min)	170	129	90
FST (min)	195	180	140

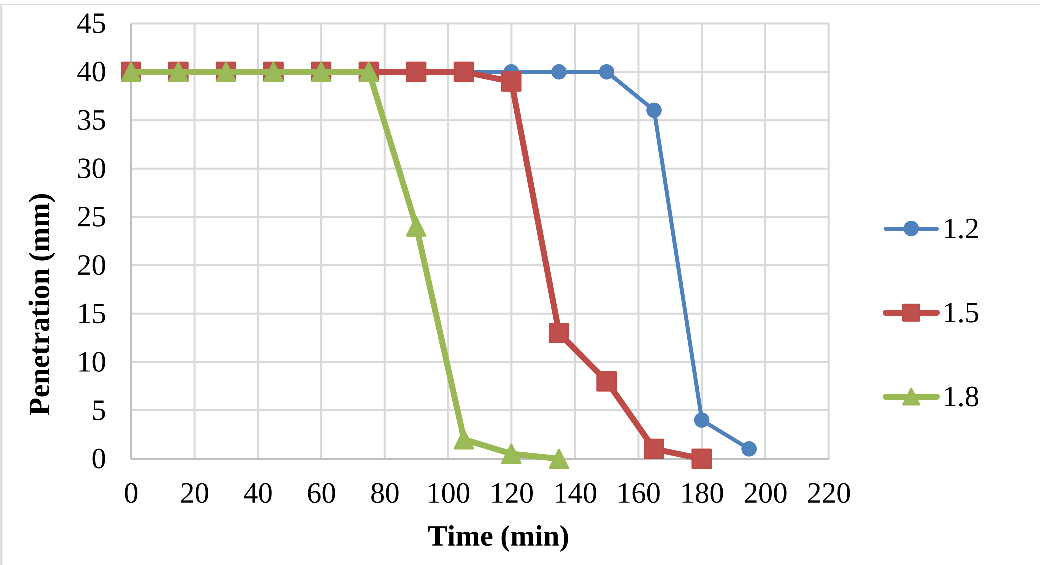

Figure 4.7: Penetration Vs. time using the hobart mixer

The mixes were evaluated using the normal concrete mixing machine. As previously mentioned, the speed of mixing is 17.5 rvm which is considered relatively slow compared to the Hobart Mixer. The *a/b* ratio 1.5 mix was the first mix to be tried on the normal mixer. Several trials had to be done to be able to achieve the optimum time for mixing. During the first trial, the mixing time for the first trial was around 20 minutes and the 0.26 *w/b* ratio was found to be not sufficient. Thus, additional water was added to achieve a homogenous mix. This water is considered 0.28 of the total volume and would require the *w/b* ratio to be readjusted from 0.26 to at least 0.40. However, this was not done and the mixing time was further increased. This led to setting-time results which are similar to the mixes mixed with Hobart mixer. The mixing time was found to be approximately 40 minutes. Another trial was performed without adding any water for water absorption. The time of mixing was increased to 60 minutes until all the clumps were broken down and a homogenous mix was achieved. This was of no good, as the IST and FST of the *a/b* ratio 1.5 mix were found to be 40 and 75, respectively, which are significantly lower than 129 and 180. Figure 4.8 demonstrates the mixing effect on the setting time results. The same mixing procedure was followed for the 1.2 and 1.8 mixes and the setting-time results were found to be similar to that of the Hobart mixer results. The open time is the time at which the mix is no longer printable. The extrudability was evaluated every 15 minutes until discontinuity was observed in the filaments. The open time of the *a/b* ratios 1.2, 1.5 and 1.8 mixes were found to be 135, 90 and 75 min, respectively, when mixed using the Hobart mixer. Note that these values are lower than the IST for the three mixes, and thus it is critical to determine the open-time of the mixes.

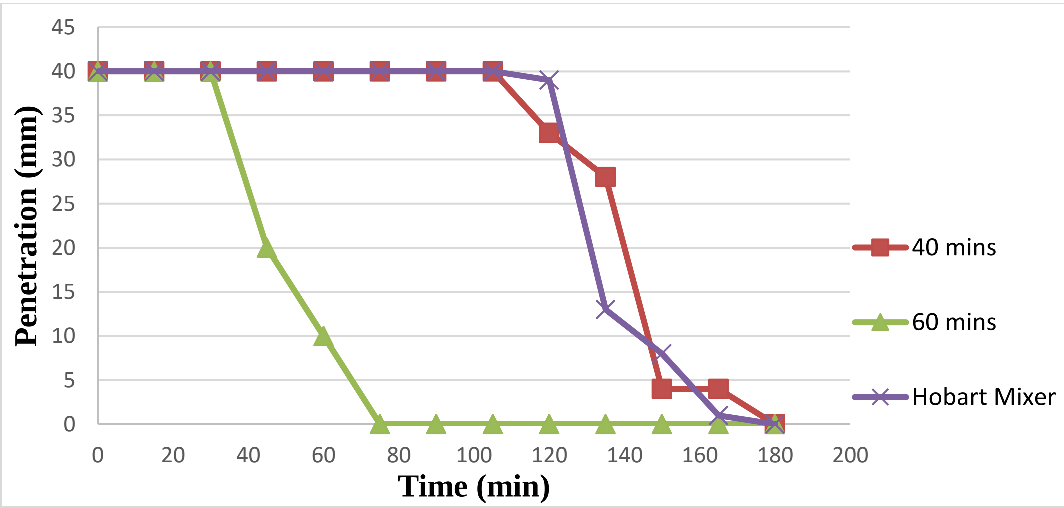

Figure 4.8: Effect of mixing on setting-time of the a/b ratio 1.5 mix

4.2.3 Comparison of workability indicators with extrudability. The Vicat penetration, slump, and flow mortar test were monitored every 15 minutes with the extrudability. The results of the *a/b* ratio 1.2, 1.5, and 1.8 mixes using the normal concrete mixing machine are summarized in Table 4.2.

Table 4.2: Summary of workability indicators of phase 2 mixes.

Mixes		**1.2**			**1.5**			**1.8**	
Time (min)	**Pent (mm)**	**Slump (mm)**	**Flow (%)**	**Pent (mm)**	**Slump (mm)**	**Flow (%)**	**Pent (mm)**	**Sump (mm)**	**Flow (%)**
0	40	80	90.6	40	45	73	40	85	89.1
15	40	80	90.6	40	40	67.8	40	90	89.1
30	40	65	86.7	40	40	68.6	40	70	82
45	40	65	85.2	40	32	60.7	40	56	76.1
60	40	55	79	40	30	55.9	40	28	58.7
75	40	50	76.7	40	25	48	40	9	50.2
90	40	28	68.3	40	5	41.2	38	0	44
105	40	18	65.2	40	0	33.3	24	0	33.4
120	40	14	60.4	33	0	X	2	0	X
135	40	5	56.4	28	0	X	0	0	X
150	40	0	49.6	8	0	X	0	0	X
165	20	0	44.3	4	0	X	0	0	X
180	15	0	44.1	2	0	X	0	0	X
195	12	0	38.7	0	0	X	0	0	X
210	10	0	X	0	0	X	0	0	X
225	6	0	X	0	0	X	0	0	X
240	0	0	X	0	0	X	0	0	X
255	0	0	X	0	0	X	0	0	X
270	0	0	X	0	0	X	0	0	X
285	0	0	X	0	0	X	0	0	X

4.2.3.1. Penetration and extrudability. The penetration and extrudability were monitored at least twice for each mix. The penetration trials of the 1.2, 1.5, and 1.8 mixes are demonstrated in Figure 4.9. The times at which failure occurred are marked in red, and the time interval for the penetration was 15 minutes. For the first trial of the 1.2 mix, the penetration was 40 mm until 150 min, after that, the penetration decreased gradually. Once the penetration decreased beyond 40 mm at 165 min, the filaments no longer satisfied the extrudability criteria. For the second trial, the extrudability was not satisfied before the decrease in penetration by 30 min at 135 min, see Figure 4.9a. As for the two trials of the 1.5 mix, discontinuity was again observed 30 min before the decrease in penetration, i.e, at 105 min, see Figure 4.9b. The 1.8 mix on the other hand showed unacceptable performance 15 min prior to the decrease in penetration at 75 min and at the penetration decrease itself at 90 min, see Figure 4.9c.

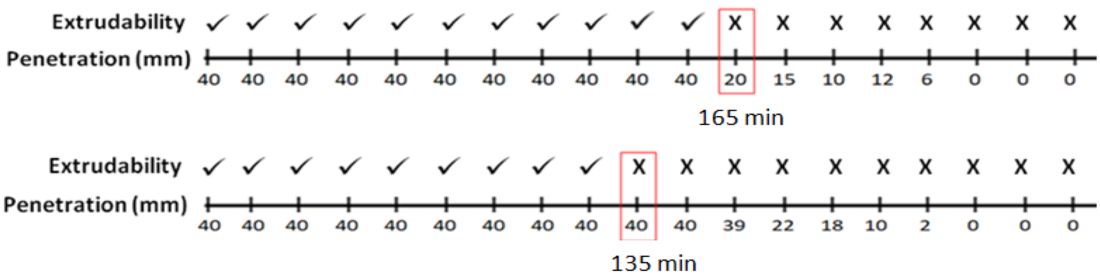

a) 1.2 Mix

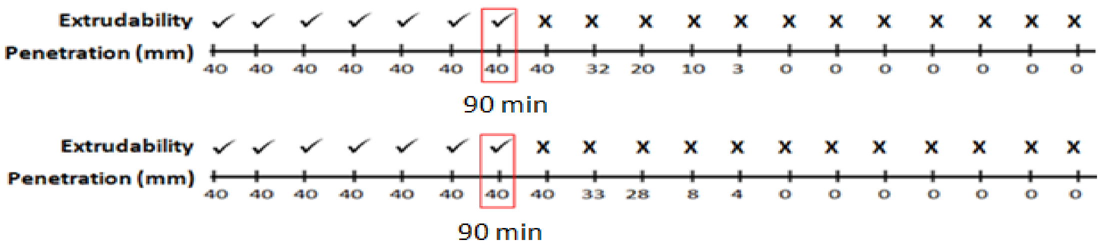

b) 1.5 Mix

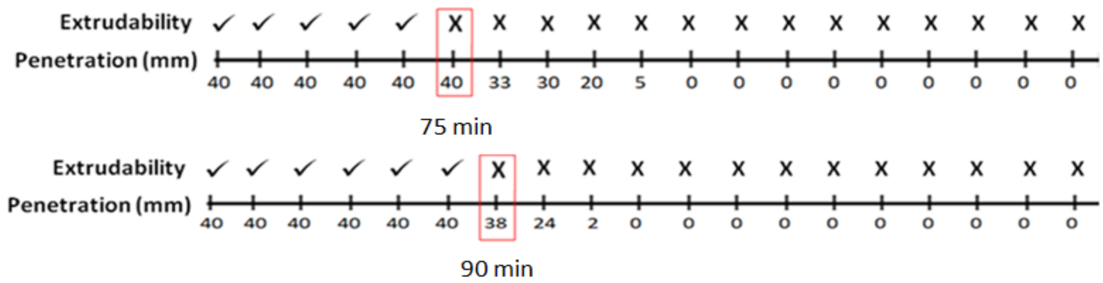

c) 1.8 Mix

Figure 4.9: Penetration for each of the 1.2, 1.5, and 1.8 mixes

The failures were mainly, inconsistency in the printed filament, and separation. As the penetration decreases beyond 40 mm with the 1 mm needle, this is an indication that the concrete has gained sufficient green strength and lost some of its plasticity which made the filaments harder to extrude and led to separation. Figure 4.10 shows a summary at which the printing quality may be affected. Note that the open time (135, 90 and 75 min) was selected to be lesser out of the two trials for each mix. The penetration versus time of the three mixes is demonstrated in Figure 4.11 from which it is observed that as the aggregate to binder ratio increases; the slope becomes steeper, indicating an increase in the rates at which the mixes are stiffening.

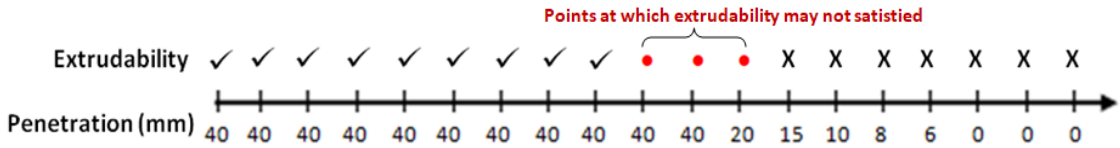

Figure 4.10: Points at which extrudability may not satisfied

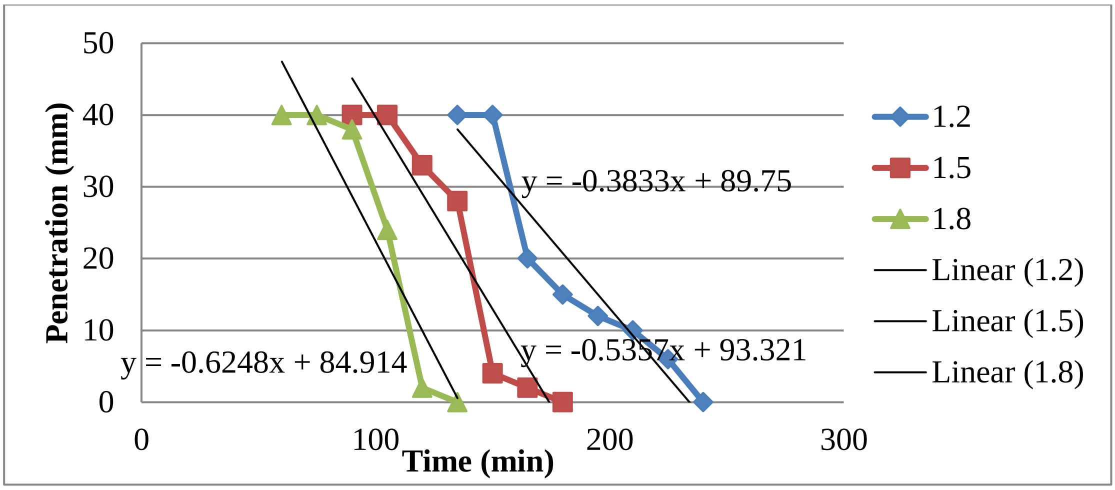

Figure 4.11: Penetration vs. time using normal concrete mixer

4.2.3.2. Slump and extrudability. The slump test was conducted every 15 minutes to evaluate the change in workability with time and to obtain the workability at which the extrudability is no longer satisfied. Figure 4.12 demonstrates the change in slump with time. As observed, at 0 min the three mixes had a slump ranging from 85 to 50 mm. The times at which the 1.2, 1.5, and 1.8 mixes were no longer extrudable were determined previously and are 135, 90, and 75 min. These values have a slump of 0, 5, and 9 mm, respectively. From the penetration results, when the extrudability was not satisfied either at the 40 mm penetration or right after it by 15 min, the slump was 0. This indicates that the slump range to satisfy the printing quality can be in the range of 85 to 0 mm. Ma et al. [51] reported that the slump range that maintained printability lied within a range of 88 to 32 mm. The upper range reported by Ma el al. was found to be quite similar to the upper range found in this study. However, for the lower range, there were times at which the 0 slump gave acceptable extrudability. From Figure 4.12 it is shown that the slopes of the 1.2, 1.5, and 1.8 mixes are -0.59, -0.42, and -1.09; respectively. The 1.5 mix shows a lower slope than that of the 1.2 mix, indicating that the structuration rate for the 1.2 is higher than that of the 1.5 mix. These results are different than the Vicat needle results, as the rate at which the mixes were stiffening was found to be increasing as the aggregate to binder ratio increases. The aggregate to binder ratio is a factor which affects the structuration rate of the mixes, and it is expected, that as the a/b ratio increases, the structuration rate should also increase. The slump results suggest that the slump test may not always give accurate results.

Additional trials were conducted to observe the slump at which the extrudability was not satisfied. It was found that when the slump exceeded 90 mm either blockage happened, or the filaments did not maintain their shape. The 0 slump on the other hand does not necessarily affect the extrudability. There were times at which the 0 slump gave acceptable extrudability and times at which the filaments were too hard to be extruded. Thus, it can be concluded from the slump results, that the slump only gives an indication of the extrudability, consistency and homogeneity of the concrete, and cannot be completely relied on to evaluate the workability of the printing concrete. Extrudability has to be within a slump ranging from 85 to 0 mm; however, it should be noted that these values will not always necessarily cause the concrete to pass the extrudability criteria and thus other test methods should be proposed to evaluate the workability of the printing concrete. Figure 4.13 demonstrates concrete with 110 mm slump which failed the extrudability criteria as well as 0 slump after the open-time of the mixes were exceeded. It is clear that at this stage the slump has lost some of its plasticity and will no longer produce concrete with acceptable printing quality. Even if the concrete was extruded, the bonding between the layers may be very weak.

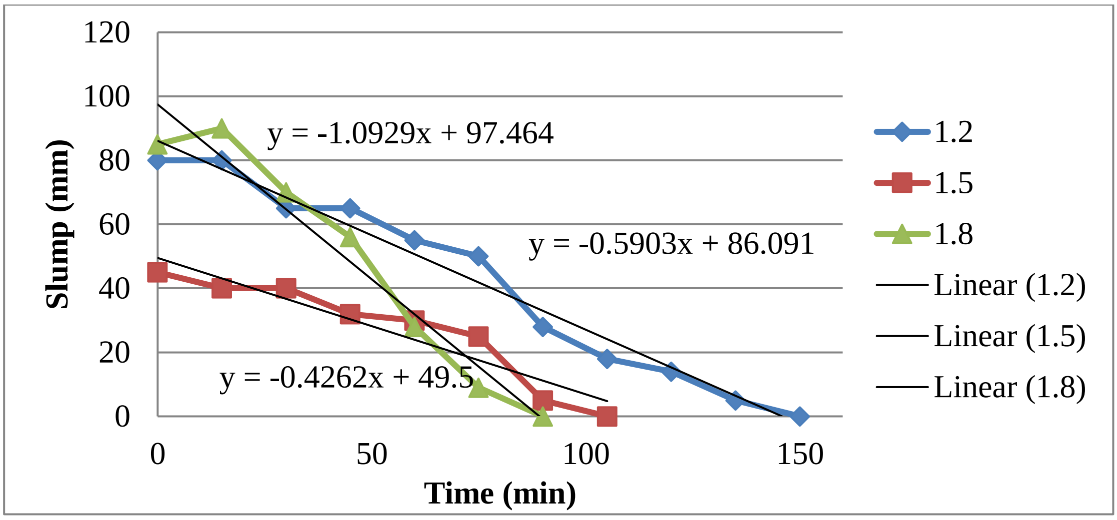

Figure 4.12: Change of slump with time

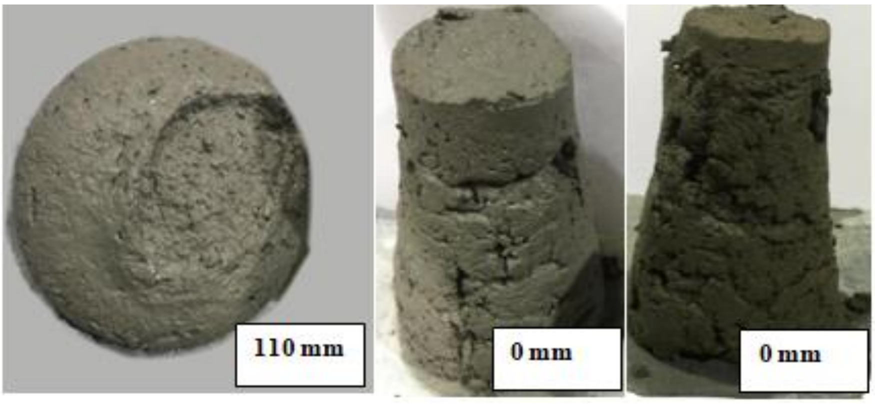

Figure 4.13: Unacceptable slump values

4.2.3.3. Flow and extrudability. Similar to the slump test, the mortar flow test was also conducted every 15 minutes. The 1.2, 1.5, and 1.8 mixes have a flow percentage ranging between 90.6-44.3 %, 73-41.2 %, and 89-44 %; respectively. Figure 4.14 shows the rate at which flow is lost with time. The 1.8 has the steepest slope of -0.58 indicating that the rate of structuration for is greatest for this mix. Similar to the Vicat penetration results, the structuration rate increases with the increase in *a/b* ratio. From the results, when the flow is around 44% and lower, the workability is affected. Additional trials were performed to evaluate the flow at which the filaments are too wet to be printed. It was found out that when the flow is beyond 95%, blockage may happen, or the filaments may be unstable and inconsistent.

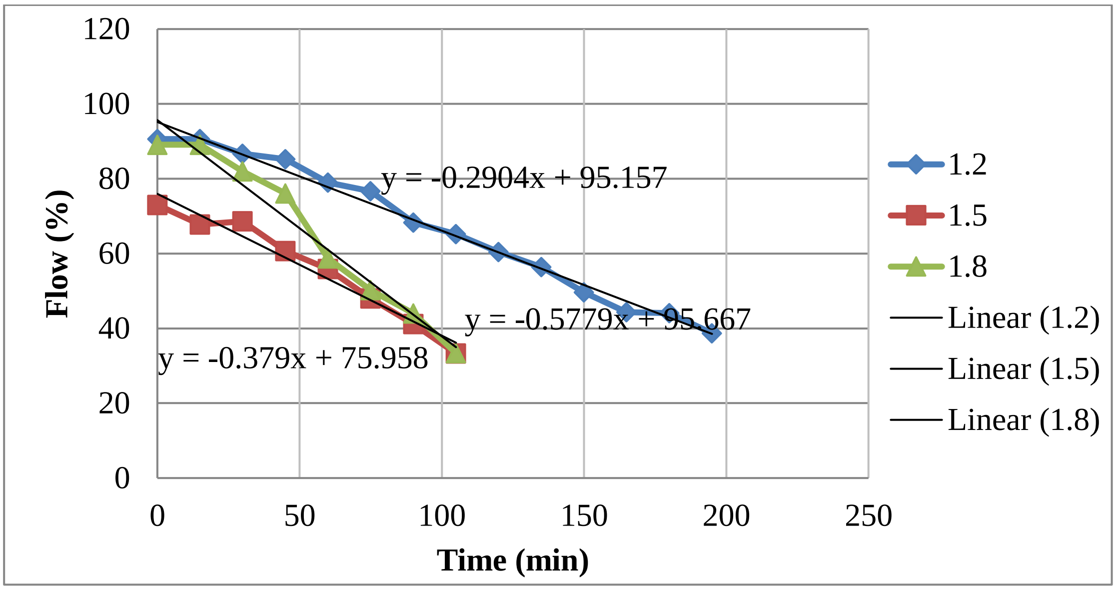

Figure 4.14: Change of flow with time

In Figure 4.15, the change in flow in mixes 1.5 and 1.8 is depicted. As observed, at 41.2% and 44%, the flow seems to be unacceptable, and either blockage or separation happen. The flow seems to give more consistent results than the slump test and gives better indication in terms of the structuration rate. Thus, the flow results were selected and a model was developed to check the effect of the aggregate to binder ratio on the percentage flow at which the extrudability is not satisfied. Figure 4.16 shows the prediction model.

a) Flow of 1.5 mix

b) Flow of 1.8 mix

Figure 4.15: Mortar flow test lab results

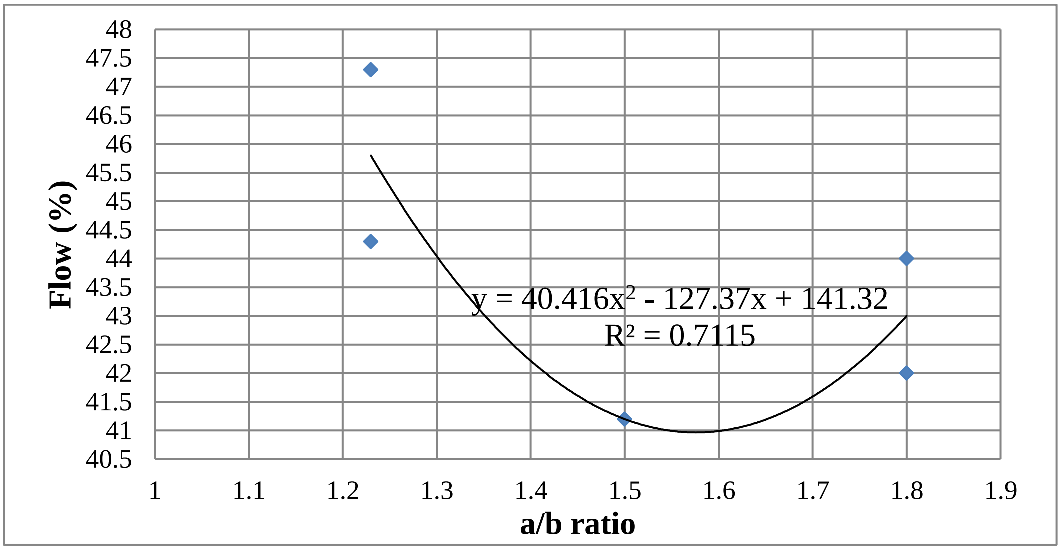

Figure 4.16: Prediction model for flow

From Figure 4.16, the coefficient of determination (R^2) is determined to be as 0.71. This value is considered relatively good and indicates that there may be 29% variation in the percentage flow. All *a/b* ratios ranging from 1.2 to 1.8 have a specific flow at which the concrete will not be printable, and this can be determined from the proposed model. For instance, a *1.55* a/b ratio mix should correspond to a 41% flow. To validate the model, two mixes of 1.3 and 1.72 a/b ratio were developed and the mortar flow test was conducted every 15 minutes until the filaments were no longer extrudable. From the experimental results, both the 1.3 and 1.72 failed at a flow of 43.2 and 41.6%. From the graph in Figure 4.16, these mixes correspond to a flow of 44 and 41.8 %. The results of both the experimental and analytical model seem to be close to each other with a percentage difference of 1.8 and 0.48 % for the 1.3 and 1.72 mixes, indicating a reliable model. More trials of different a/b ratios are suggested to further validate the accuracy of the model.

4.2.3.4. Pearson correlation analysis. Pearson Correlation analysis is a statistics test which determines the statistical relationship or association between two continuous variables. This method was adopted to find the relationship and its strength between each of the workability indicators with time as well as their mutual relationships to confirm the findings of the study. Tables 4.3 to 4.5, demonstrate the Pearson Correlation Coefficient of each of the 1.2, 1.5, and 1.8 mixes. The correlation analysis discussion will be as follows. The strength of the relationship of each parameter, penetration, slump, and flow, with time will first be presented, followed by the mutual correlation of each workability indicators.

While comparing each of the variables with time, all the coefficients have a negative value, indicating that as time increases, there is a loss in workability. Flow has the strongest relationship with time as the mixes have coefficients ranging from 0.98 to 0.99, followed by the penetration and slump which have coefficients ranging from 0.87 to 0.91, and 0.76 to 0.89. Slump has the lowest relationship with time when compared to the penetration and flow. The structuration rate of each of the 1.2, 1.5, and 1.8 mixes was previously indicated by the slopes of each of the penetration, slump, and flow with time (Figures 4.11, 4.12, and 4.14). Based on the slopes of the penetration and flow, the structuration rate was found to be increasing as the a/b ratio increases. However, the slump showed that the 1.5 mix had a lower structuration rate than that of the 1.2 mix. The structuration rate of each of these variables was determined by change of each of the penetration, slump, and flow with time, and thus each of these variables should have a strong correlation with time to be considered as an indicator for both flowability and structuration. From the correlation analysis performed, the slump had the lowest correlation with time when compared to the flow and penetration. This indicates that the structuration rates obtained from the slump results may be less accurate than the rates obtained from the penetration and flow. Based on the statistical analysis, it is observed that the flow test would give the best indication of structuration followed by the penetration and slump.

The penetration-slump, penetration-flow, and slump-flow relationship strengths showed a correlation of 0.67 to 0.73, 0.65-0.72, and 0.97-0.98, respectively. The penetration seems to have the lowest correlation when compared to either the flow or slump. Even though the penetration showed the lowest coefficients, this relationship is still considered as good as the values are greater than 0.6. The slump-flow on the other hand are considered to have a very strong relationship. Overall, all variables were observed to have a very strong relationships with time. The flow test showed the strongest relationship with time with a correlation coefficient of 0.99. The flow test gives an indication of the change of viscosity of the fresh concrete with time, and thus it is rational that the flow test would give the highest correlation. Since extrudability is a time dependent factor, the flow test is expected to give the most accurate results for extrudability when compared to either the penetration test or the slump.

Table 4.3: Pearson correlation coefficients for the 1.2 Mix

	Time	**Penetration**	**Slump**	**Flow**
Time	1.000	-0.907	-0.891	-0.993
Penetration	-0.907	1.000	0.674	0.721
Slump	-0.891	0.674	1.000	0.970
Flow	-0.993	0.721	0.970	1.000

Table 4.4: Pearson correlation coefficients for the 1.5 Mix

	Time	**Penetration**	**Slump**	**Flow**
Time	1.000	-0.906	-0.825	-0.982
Penetration	-0.906	1.000	0.715	-
Slump	-0.825	0.715	1.000	0.976
Flow	-0.982	-	0.976	1.000

Table 4.5: Pearson correlation coefficients for the 1.8 Mix

	Time	Penetration	Slump	Flow
Time	1.000	-0.869	-0.757	-0.982
Penetration	-0.869	1.000	0.736	0.653
Slump	-0.757	0.736	1.000	0.983
Flow	-0.982	0.653	0.983	1.000

4.2.4 Buildability. Buildability was performed for the 3 mixes using both the circular and square nozzle. Buildability is dependent on all the factors that affect the structuration rate as well as the shape of the layers which plays a role providing stability to the structure. The factors that affect the structuration rate are the mix proportions, *a/b* and *w/b* ratios, materials used, and additives. Each of these have a significant impact on the buildability. Regardless of the nozzle shape used, the increase in *a/b* ratio increased the buildability. Initially, when the first layer of each of the 1.2, 1.5, and 1.8 mixes was extruded, all the filaments had the same workability, i.e. green strength. The difference in the buildability cannot be witnessed during the first couple of minutes if all the three mixes had the same workability. However, as time increases beyond few 10s of minutes, the rate of structuration (thixotropy) will play a role, and the layers of the mixes with lower a/b ratio will lose their shape stability upon extrusion as they have lower structuration rates. For this study, within the first 20 min all mixes were observed to have the same number of layers using the square nozzle. After approximately 20 minutes, the buildability for each mix was varied.

As previously stated, based on the penetration and flow results, the structuration rate was highest for the 1.8 mix, followed by the 1.5, and 1.2 mixes. From these results, it is expected for the 1.8 mix to have the highest number of layers within the shortest time since it has the highest structuration rate. Note that the filaments were extruded continuously above each other from the same batch with a time gap of approximately 1-2 minutes. The 1.8 showed the best performance followed by the 1.5 and 1.2. The maximum number of layers reached by the circular nozzle was 10. External supports were required to go beyond 10 layers, this is because circular nozzles in general do not provide good shape stability and have low area of contact compared to square and rectangular nozzles. The buildability of the circular nozzle of each of the 1.2, 1.5, and 1.8 mix is demonstrated in Figure 4.17.

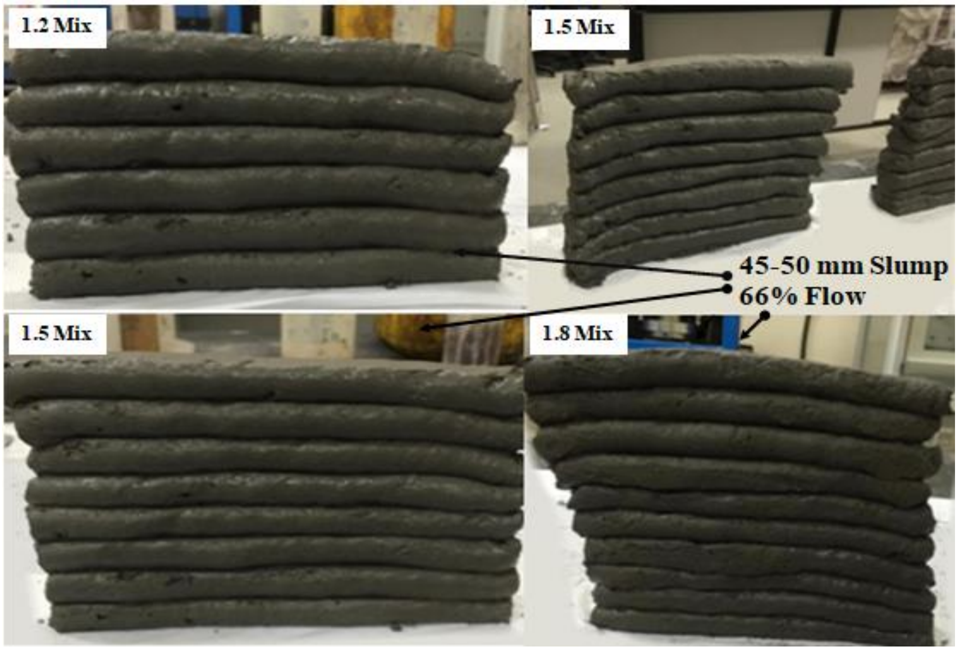

Figure 4.17: Buildability of the 1.2, 1.5, and 1.8 mixes using the circular nozzle

The computed slump and flow range to maintain printability was found to be within the ranges of 85 to 0 mm and 90.6 to 45 %. Note that the 85 mm slump and 90.6% give good extrudability performance but do not satisfy the buildability requirement. Thus, it is necessary to determine the slump and flow values which would satisfy both the extrudability and buildability criteria. Before layering the filaments above each other, the slump and flow was first determined to check the workability with the number of layers. The buildability demonstrated in Figures 4.17-4.19 corresponds to slump and flow ranges of 45-55 mm and 66-60%, respectively. The 85 mm slump and 90.6% flow could be used with the use of accelerators to increase the structuration rate of the mix and to satisfy the buildability. The workability of the mixes used in this study was adjusted to be within these ranges of 45-55 mm slump and 66-60 % flow and accelerators were not added. The 20x20 mm square nozzle produced more stable filaments compared to the 17 mm circular nozzle. The buildability of the square nozzle for the 3 mixes is shown in Figure 4.18. For the 1.2 mix, up to 10 layers were reached, after that, due to the pressure of the above layers on the first layers, the shape became unstable and external supports had to be used to further proceed. The 1.5 mix reached up to 11 layers, and again external supports had to be used. As for the 1.8 mix, up to 15 layers were reached without external supports and no failure occurred, see Figure 4.19.

Note that if a wider rectangular nozzle was used, the 1.2 and 1.5 mixes would not have required external supports. The buildability results suggest that if the time gap between the layers of the 1.2 and 1.5 mixes was higher than 1-2 min, the buildability performance for these mixes would have been better due to the increase in structural rebuilding rate with time. Thus, it is very critical for the number of layers to be monitored with the structural rebuilding rate.

Figure 4.18: Buildability of the 1.2, 1.5, and 1.8 mixes using the square nozzle

Figure 4.19: Buildability of the 1.8 mix with 15 Layers

4.2.5 Compressive strength. The compressive strength of the cast specimens of the 1.2, 1.5 and 1.8 mixes, were 33, 34, and 34.5 MPa at 3 days, and 44.3, 52, and 53.8 MPa at 28 days. As observed, the compressive strength increases with the increase in *a/b* ratio. In Figure 4.20 the testing of the 3x3 layer cube is illustrated. The compressive strength of the cast and printed specimens at 3 days is presented in Figure 4.21. The printed specimens were only tested in the perpendicular direction. From the literature, the longitudinal direction is considered the strongest direction amongst the lateral and perpendicular direction.

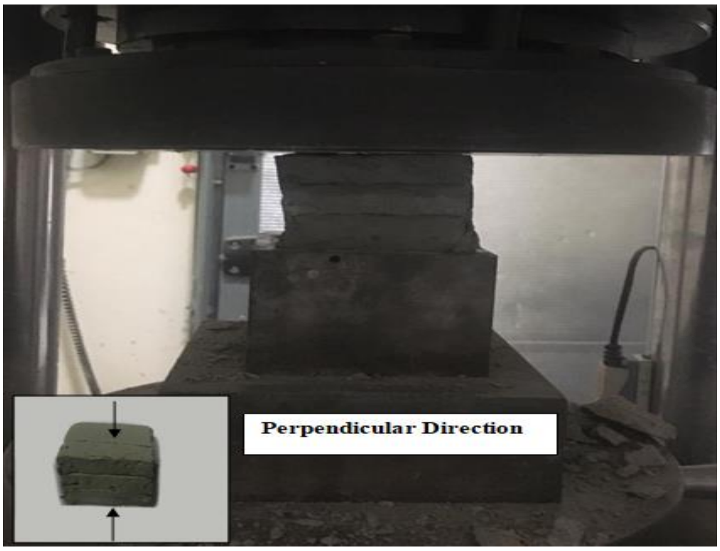

Figure 4.20: Compression strength test set up

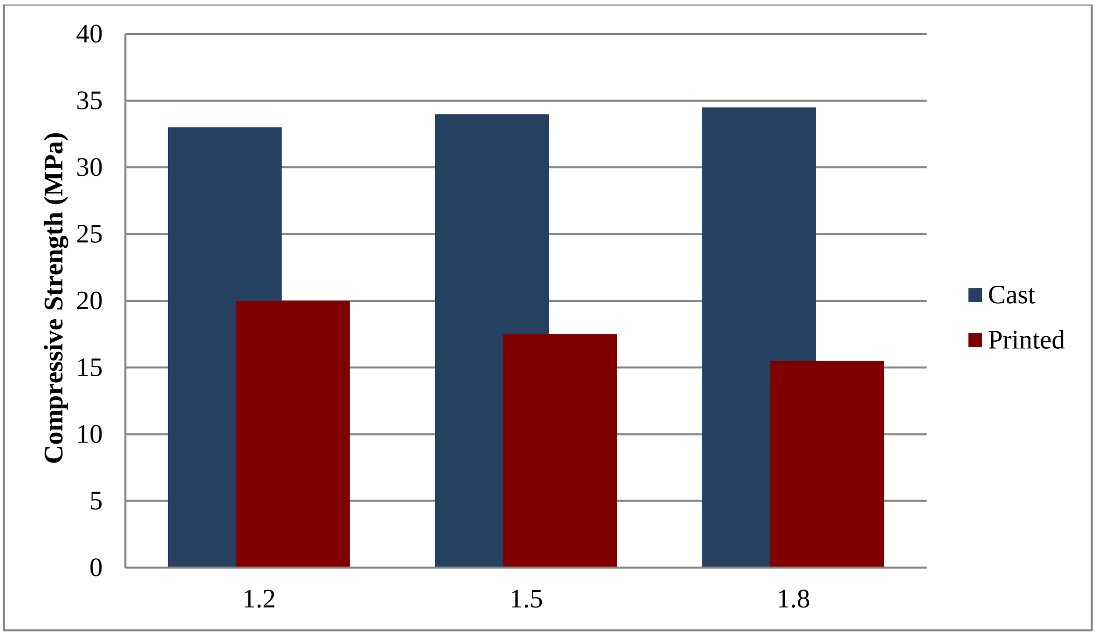

Figure 4.21: Compression strength of cast and printed specimens at 3 Days

For the printed specimens, the compressive strength was decreasing with the increase in the *a/b* ratio. These results are not similar to that of the cast specimens. In printing concrete, the interlayer bond strength is the most important property that will affect the mechanical properties of the concrete. As the *a/b* ratio increases, the bond strength between the layers decreases. The 1.8 mix had the highest structuration rate (thixotropy) which was previously observed from the workability results. Even though a high thixotropy is usually preferred for printing concrete, it has been found out that this may lead to weak bonding between the layers and cause cold joints [41]. The increase in thixotropy observed in the mixes may have led the strengths to decrease with the increase in the *a/b* ratio. The failure modes of the printed specimens were found to be similar to that of the cast specimens. The failure modes of some of the printed specimens of the 1.2 and 1.5 mixes are shown in Figure 4.22.

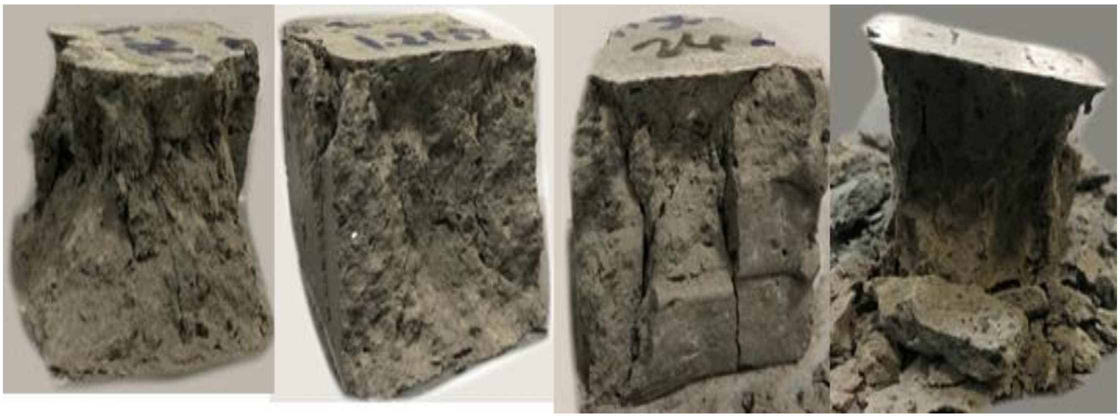

Figure 4.22: Failure modes of 3x3 layer printed specimens of 1.2 and 1.5 mixes.

4.2.6 Summary of phase 2 mixes. A summary of all the setting-time, open time, workability, buildability and compressive strength results of the 1.2, 1.5, and 1.8 mixes are presented in Table 4.6. From the results, it is observed that the setting-time and open-time decrease with the increase in a/b ratio. For the buildability and compressive strength, the result show that as the a/b ratio increased, the buildability also increased; however, the compressive strength decreased. These results suggest that the 1.2 mix is best in terms of the open time and compressive strength, and thus it is suggested to further enhance this mix by adding fibers.

Table 4.6: Summary of the properties of phase 2 mixes

	Mixes		
	1.2	**1.5**	**1.8**
Fresh Properties			
Setting-time (min)	170	129	90
Open-time (min)	135	90	75
Workability to satisfy extrudability criteria			
Slump (mm)	80-0	45-5	85-0
Flow (%)	90.6-44.3	73-41.2	89.1-44
Workability used for buildability criteria			
Slump (mm)		45-50	
Flow (%)		66-60	
Buildability			
No. of Layers using Circular Nozzle	6	8	10
No. of Layers using Square Nozzle	10	11	15
Compressive Strength (MPa)			
Cast Specimens at 3 Days	33	34	34.5
Cast Specimens at 28 Days	44.3	52	53.8
Printed Specimens at 3 days. (Tested in Perpendicular Direction)	20	17.5	15.5

Chapter 5. Conclusion and Recommendations

The aim of this study was to develop a 3D printing concrete and to assess it in terms of extrudability, workability, setting-time, buildability and compressive strength. The experimental program was divided into two phases. The first phase involved developing a printing concrete. First, two groups of mixes were developed to evaluate the effect of the different supplementary materials on the extrudability of the printing concrete as well as the compressive strength of cast specimens. Then, the optimal mix from phase 1 evaluation was selected for phase 2 evaluation, and was assessed in terms of the extrudability, workability, setting-time, buildability and compressive strength.

The two groups of phase 1 evaluation consisted of exactly the same binding materials, the only difference was that Group I mixes consisted only of dune sand and Group II mixes consisted of a blend of both dune and crushed sand. Each group consisted of four mixes, a control mix, a mix with GGBS, SF, and GGBS and SF combined. The summary of the findings of phase 1 evaluation are as follows:

1. The use of VMA is essential to adjust the extrudability of mixes containing only cement and GGBS. If VMAs are not used, bleeding or segregating may occur while adjusting the printability of the printing concrete.
2. The GGBS slightly enhanced the extrudability performance whereas the SF significantly enhanced the pumpability of the concrete which led to better extrudability results. The use of VMA is not essential when SF is used.
3. The extrusion process of mixes with crushed sand was better when compared to mixes containing dune sand only. This could be attributed to the smooth gradation curve when dune sand and crushed sand are used as fine aggregate.

The optimal mix of phase 1 (DC-GBSF) was selected and was developed with three different aggregate to binder ratios of 1.2, 1.5, and 1.8 for phase 2 evaluation. The workability was assessed in terms of penetration, slump, and flow, and was conducted every 15 minutes to monitor the extrudability with time. Two types of mixers were used in this evaluation which are the Hobart mixer and the normal concrete mixer. The normal concrete mixer was mainly used to satisfy the concrete volume required to test the workability with time. The outcomes of phase 2 evaluation can be summarized as follows:

1. The open-time of the 1.2, 1.5, and 1.8 mixes was found to be 135, 90 and 60 min which is less than the 170, 129, and 90 min initial setting-time.
2. The mixing time for the Hobart mixer was only 5 minutes, whereas, for the normal concrete mixer due to the low speed, several trials had to be done to obtain the optimum time of mixing and to achieve the same setting-time results of the Hobart mixer. The optimal time using the normal concrete mixer was found to be 40 minutes.
3. As for the workability evaluation with time. The penetration and mortar flow test both indicated that as the aggregate to binder ratio increases the structuration rate (thixotropy) of the mixes also increase. The slump on the other hand showed that the 1.5 mix had a lower structuration rate than that of the 1.2. Since the structuration rate is dependent on time, correlation analysis was performed to determine the correlation between each of these factors with time, and it was found out that both the penetration and mortar have a stronger relationship with time as compared to the slump for the three mixes.
4. The extrudability for the penetration was not satisfied in either one of the following: 1) 30 min before the first penetration decrease, 2) 15 min before the first penetration decrease, and 3) at the penetration decrease itself. As for the slump and flow, the ranges that maintain acceptable extrudability are 85-0 mm slump and 90-45 % flow.
5. The flow showed the strongest correlation of 0.99 with time. Since, extrudability is time dependent, it is suggested that the flow gives the best indication of extrudability when compared to the slump and penetration. The slump may only give an indication of the buildability and cannot be completely relied on.
6. A prediction model was developed to determine the flow at which the printability will not be satisfied for different aggregate to binder ratios. The R^2 was found to be 0.71 which is considered relatively good. To verify the model, two mixes of 1.3 and 1.72 a/b ratios were tried, and failure occurred at a flow of 43.2 and 41.6% which are close to 44 and 41.8 % obtained from the graph.

7. The buildability increased with the increase in a/b ratio, given that the workability of all the mixes had to be adjusted to be the same. The workability for buildability was adjusted to be 45-50 mm slump and 66% flow.
8. Even though the buildability enhanced with the increase in a/b ratio, the compressive strength decreased with the increase in a/b ratio which is probably due to the increased thixotropy observed from the penetration, slump and flow results. The compressive strength of the printed specimens was around 50% less than that of the cast (vibrated) specimens at 3 days when tested only in the perpendicular direction.

As observed, the workability of the printing concrete in this research was only assessed by the penetration, slump and flow over time through which an indication of the structuration rate was presented. The flow gave the best indication of the rheology of concrete, and thus it would be interesting to study the correlation between the rheological properties (yield stress, viscosity and thixotropy) with the flow. For the setting time, a trend between the penetration and extrudability was observed and thus it is suggested to find the relationship between the penetration resistance and extrudability using other penetration tests. In general, the slump cone dimensions of (50, 100, and 150) seem to give satisfactory results in terms of the slump. Since the interlayer strength is one of the most vital properties that affect the mechanical properties of the concrete, the optimal ranges of both the slump and mortar should take this into account. For instance, a 0 slump is likely not to give the same bond strength as a 60 mm slump. The buildability is highly dependent on the structuration rate of the concrete, and thus it is very essential to monitor the structuration rate to determine the optimal time that would avoid the collapse of the layers. External temporary supports may sometimes be used until the concrete has gained sufficient strength to solve some of the buildability issues. Also, the interlayer strength has to be studied with time and all the factors that affect it should be studied as this is one of major challenges of printing concrete.

References

[1] R. O. Asamoah, J. S. Ankrah, K. Offei-Nyako, and E. O. Tutu, "Cost Analysis of Precast and Cast-in-Place Concrete Construction for Selected Public Buildings in Ghana," *Journal of Construction Engineering,* vol. 2016, pp. 1-10, 2016.

[2] K. Jones. "Construction Leads All Industries in Total Worker Deaths." https://www.constructconnect.com/blog/construction-news/construction-leads-industries-worker-deaths/ (accessed September 16, 2019).

[3] E. Worrell, L. Price, N. Martin, C. Hendriks, and L. O. Meida, "Carbon dioxide emissions from the global cement industry," *Annual Review of Energy and the Environment,* vol. 26, no. 1, pp. 303-329, 2001.

[4] A. M. Forster, "Materials testing standards for additive manufacturing of polymer materials," *NI: ST, Department of Commerce,* 2015.

[5] J. Pegna, "Exploratory investigation of solid freeform construction," *Automation in Construction,* vol. 5, no. 5, pp. 427-437, 1997.

[6] D. Hwang and B. Khoshnevis, "An innovative construction process-contour crafting (CC)," in *22nd International Symposium on Automation and Robotics in Construction ISARC 2005*, 2005, pp. 1-6.

[7] B. Khoshnevis, "Automated construction by contour crafting—related robotics and information technologies," *Automation in Construction,* vol. 13, no. 1, pp. 5-19, 2004.

[8] "D-shape." https://d-shape.com/ (accessed November 1, 2019).

[9] "3D Printing Industry." https://www.3dprintingindustry.com/news/branch-technology-is-3d-printing-the-future-of-construction-one-wall-at-a-time-54149 (accessed January 10, 2018).

[10] L. Novakova-Marcincinova, "Application of fused deposition modeling technology in 3D printing rapid prototyping area," *Manuf. and Ind. Eng,* vol. 11, no. 4, pp. 35-37, 2012.

[11] L. Feng and L. Yuhong, "Study on the Status Quo and Problems of 3D Printed Buildings in China," *Global Journal of Human-Social Science Research,* 2014.

[12] "China building world's largest 3D printer to construct houses." http://www.3ders.org/articles/20140625-china-building-world-largest-3d-printer-to-construct-houses.html (accessed November 5, 2019).

[13] http://www.constructionmanagermagazine.com/news/chinese-firm-unveils-worlds-largest-3d-printer/ (accessed November 5, 2019).

[14] "Xinkebot." http://www.xinkebot.com/en/nd.jsp?_np=103_420&id=220 (accessed January 15, 2018).

[15] *Contour Crafting*. Available: http://contourcrafting.com/building-construction/ (accessed November 6, 2019).

[16] G. Ma, L. Wang, and Y. Ju, "State-of-the-art of 3D printing technology of cementitious material—An emerging technique for construction," *Science China Technological Sciences,* vol. 61, pp. 1-21, 2017.

[17] A. rudenko. "andrey rudenko constructs 3D printed concrete castle in minnesota." https://www.designboom.com/technology/3d-printed-concrete-castle-minnesota-andrey-rudenko-08-28-2014/ (accessed January 10, 2018).

[18] M. Starr. "World's first 3D-printed apartment building constructed in China." https://www.cnet.com/news/worlds-first-3d-printed-apartment-building-constructed-in-china/ (accessed November 12, 2019).

[19] "The World's First 3D Printed Office." http://www.officeofthefuture.ae/# (accessed November 14, 2019).

[20] "3D Printed Office." http://www.officeofthefuture.ae/# (accessed November 13, 2019).

[21] J. Belezina. "D-Shape 3D printer can print full-sized houses." https://newatlas.com/d-shape-3d-printer/21594/ (accessed November 14, 2019).

[22] F. Bos, R. Wolfs, Z. Ahmed, and T. Salet, "Additive manufacturing of concrete in construction: potentials and challenges of 3D concrete printing," *Virtual and Physical Prototyping,* vol. 11, no. 3, pp. 209-225, 2016.

[23] G. Cesaretti, E. Dini, X. De Kestelier, V. Colla, and L. Pambaguian, "Building components for an outpost on the Lunar soil by means of a novel 3D printing technology," *Acta Astronautica,* vol. 93, pp. 430-450, 2014.

[24] S. Lim, R. A. Buswell, T. T. Le, S. A. Austin, A. G. Gibb, and T. Thorpe, "Developments in construction-scale additive manufacturing processes," *Automation in construction,* vol. 21, pp. 262-268, 2012.

[25] T. T. Le, S. A. Austin, S. Lim, R. A. Buswell, A. G. Gibb, and T. Thorpe, "Mix design and fresh properties for high-performance printing concrete," *Materials and structures,* vol. 45, no. 8, pp. 1221-1232, 2012.

[26] S. Lim, R. A. Buswell, P. J. Valentine, D. Piker, S. A. Austin, and X. De Kestelier, "Modelling curved-layered printing paths for fabricating large-scale construction components," *Additive Manufacturing,* vol. 12, pp. 216-230, 2016.

[27] "Dubai 3D printing Strategy." https://www.dubaifuture.gov.ae/our-initiatives/dubai-3d-printing-strategy/ <br style="mso-special-character: (accessed November 14, 2019).

[28] "How 3D Printing is Impacting the Construction Industry in UAE and Globally." https://www.concreative.me/technology (accessed November 16, 2019).

[29] "Concreative Technology." margin-bottom:12.55pt background:white"> https://www.concreative.me/technology (accessed January 10, 2018).

[30] "ACCIONA opens 3D printing construction center in Dubai." https://3dprintingindustry.com/news/acciona-opens-3d-printing-construction-center-in-dubai-164073/ (accessed November 15, 2019).

[31] "HE Saeed Mohammed Al Tayer Visits 3D-Printed Lab at Mohammed bin Rashid Al Maktoum Solar Park." https://www.dewa.gov.ae/en/about-us/media-publications/latest-news/2017/07/he-saeed-mohammed-al-tayer-visits-3d-printed-lab-at-mohammed-bin-rashid-al-maktoum-solar-park (accessed November 15, 2019).

[32] "Dubai unveils world's largest 3D printed two-storey building." https://www.thenational.ae/uae/government/dubai-unveils-world-s-largest-3d-printed-two-storey-building-1.927590#3 (accessed November 16, 2019).

[33] "CyBe Construction selected to 3D print houses in Sharjah, UAE." https://www.3dprintingmedia.network/cybe-construction-3d-print-houses-sharjah-uae/ (accessed November 16, 2019).

[34] Z. Malaeb, H. Hachem, A. Tourbah, T. Maalouf, N. Zarwi, and F. Hamzeh, "3D Concrete Printing: Machine and mix design," *International Journal of Civil Engineering,* vol. 6, no. 6, pp. 14-22, 2015.

[35] A. Perrot, D. Rangeard, and A. Pierre, "Structural built-up of cement-based materials used for 3D-printing extrusion techniques," *Materials and Structures,* vol. 49, no. 4, pp. 1213-1220, 2016.

[36] A. Kazemian, X. Yuan, E. Cochran, and B. Khoshnevis, "Cementitious materials for construction-scale 3D printing: Laboratory testing of fresh printing mixture," *Construction and Building Materials,* vol. 145, pp. 639-647, 2017.

[37] Z. Quanji, "Thixotropic behavior of cement-based materials: effect of clay and cement types," 2010.

[38] B. Zareiyan and B. Khoshnevis, "Effects of interlocking on interlayer adhesion and strength of structures in 3D printing of concrete," *Automation in Construction,* vol. 83, pp. 212-221, 2017.

[39] Y. Zhang, Y. Zhang, W. She, L. Yang, G. Liu, and Y. Yang, "Rheological and harden properties of the high-thixotropy 3D printing concrete," *Construction and Building Materials,* vol. 201, pp. 278-285, 2019.

[40] B. Panda, G. B. Singh, C. Unluer, and M. J. Tan, "Synthesis and characterization of one-part geopolymers for extrusion based 3D concrete printing," *Journal of Cleaner Production,* vol. 220, pp. 610-619, 2019.

[41] N. Roussel, "Rheological requirements for printable concretes," *Cement and Concrete Research,* vol. 112, pp. 76-85, 2018.

[42] J. Hu, "A study of effects of aggregate on concrete rheology," 2005.

[43] H. Beushausen and M. Alexander, "Bond strength development between concretes of different ages," *Magazine of Concrete Research,* vol. 60, no. 1, pp. 65-74, 2008.

[44] R. W. Gillette, "Performance of Bonded Concrete Overlays," in *ACI Materials Journal*, 1963, vol. 60, no. 1, pp. 39-50.

[45] S. Austin, P. Robins, and Y. Pan, "Tensile bond testing of concrete repairs," *Materials and Structures*, vol. 28, no. 5, p. 249, 1995.

[46] T. T. Le *et al.*, "Hardened properties of high-performance printing concrete," *Cement and Concrete Research,* vol. 42, no. 3, pp. 558-566, 2012.

[47] J. G. Sanjayan, B. Nematollahi, M. Xia, and T. Marchment, "Effect of surface moisture on inter-layer strength of 3D printed concrete," *Construction and Building Materials,* vol. 172, pp. 468-475, 2018.

[48] P. Feng, X. Meng, J.-F. Chen, and L. Ye, "Mechanical properties of structures 3D printed with cementitious powders," *Construction and Building Materials,* vol. 93, pp. 486-497, 2015.

[49] V. Nerella, M. Krause, M. Näther, and V. Mechtcherine, "Studying printability of fresh concrete for formwork free concrete on-site 3D printing technology (CONPrint3D)," in *Proceeding for the 25th conference on rheology of building materials,* 2016.

[50] B. Rongbing and S. Jian, "Synthesis and evaluation of shrinkage-reducing admixture for cementitious materials," *Cement and Concrete Research,* vol. 35, no. 3, pp. 445-448, 2005.

[51] G. Ma, Z. Li, and L. Wang, "Printable properties of cementitious material containing copper tailings for extrusion based 3D printing," *Construction and Building Materials,* vol. 162, pp. 613-627, 2018.

[52] K. H. Khayat and Z. Guizani, "Use of viscosity-modifying admixture to enhance stability of fluid concrete," *Materials Journal,* vol. 94, no. 4, pp. 332-340, 1997.
[53] D. Suresh and K. Nagaraju, "Ground granulated blast slag (GGBS) in concrete–a review," *IOSR Journal of Mechanical and Civil Engineering,* vol. 12, no. 4, pp. 76-82, 2015.
[54] B. Langan, K. Weng, and M. Ward, "Effect of silica fume and fly ash on heat of hydration of Portland cement," *Cement and Concrete Research,* vol. 32, no. 7, pp. 1045-1051, 2002.

Vita

Sara Khaled Ahmed was born in 1995, in Cairo, Egypt. She received her primary and secondary education in Al Ain, UAE. She received her B.Sc. degree in Civil Engineering from the American University of Sharjah in 2016.

In September 2017, Sara joined the Civil Engineering master's program in the American University of Sharjah. During her master's study, she worked as a graduate teaching and research assistant through which she gained teaching and research related experience. Sara participated in several conferences. Her research interests are mainly in material and structural engineering.